

Efficient Stochastic Optimal Control through Approximate Bayesian Input Inference

Joe Watson, Hany Abdulsamad, Rolf Findeisen, *Member, IEEE*, and Jan Peters, *Fellow, IEEE*

Abstract—Optimal control under uncertainty is a prevailing challenge for many reasons. One of the critical difficulties lies in producing tractable solutions for the underlying stochastic optimization problem. We show how advanced approximate inference techniques can be used to handle the statistical approximations principled and practically by framing the control problem as a problem of input estimation. Analyzing the Gaussian setting, we present an inference-based solver that is effective in stochastic and deterministic settings and was found to be superior to popular baselines on nonlinear simulated tasks. We draw connections that relate this inference formulation to previous approaches for stochastic optimal control and outline several advantages that this inference view brings due to its statistical nature.

Index Terms—Stochastic Optimal Control, Trajectory Optimization, Covariance Control, Approximate Inference

I. INTRODUCTION

Control-as-inference [1]–[4] refers to the formulation of optimal control as inference of an equivalent probabilistic graphical model. The motivation for this perspective is threefold: Firstly, it allows one to derive intriguing mathematical dualities between the field of control and probabilistic inference, which has captivated researchers for decades [5]–[7]. Secondly, in making the effort to reframe the optimal control problem as one of Bayesian inference, we gain access to a sophisticated suite of tools and insights developed by the statistics community that provides value in both theory and practice [8]. In particular, as stochasticity presents a challenge in designing tractable algorithms for control under uncertainty [9], approximate inference techniques [10] provide means of obtaining distributions through principled approximations. Finally, an abundance of data, combined with the pervasive demand for sophisticated control design, has driven the study of *learning* for control, where experience is leveraged within the control optimization process [11]–[13]. In this setting, the motivation of inference-based optimal control is clear, as an inference-based formulation is complementary to a learned probabilistic dynamics model. Using the language of inference, optimal control and data can be integrated directly to synthesize effective control learning algorithms [14].

This project has received funding from the European Union's Horizon 2020 program under grant agreement No #640554 (SKILLS4ROBOTS). J. Watson and J. Peters are with the Intelligent Autonomous Systems group, Technical University of Darmstadt. H. Abdulsamad is with the Finnish Centre of AI and the Electrical Engineering and Automation Department, Aalto University. R. Findeisen is with the Control and Cyber-Physical Systems Laboratory, Technical University of Darmstadt. Contact: {joe, hany, jan}@robot-learning.de, rolf.findeisen@tu-darmstadt.de.

Taking the inference perspective, this article concerns the application of Bayesian smoothing methods for optimal control, focusing on the Gaussian setting [15]–[17]. Specifically, this work builds on the view of optimal control as the problem of input estimation [18], developing the seminal work reformulating approximate optimal control as approximate message passing on a probabilistic graphical model [15], [19]. Rather than using the regularized Riccati equation updates [15], we leverage the inference duality and perform optimization as a Bayesian smoothing problem in the state-action space. This view provides an alternative to linearization-based nonlinear optimal control and yields accurate, regularized estimates of the value functions using approximate inference. Moreover, inspired by inference of state-space models, we propose an expectation maximization scheme that enables the optimization of priors and hyperparameters, which is beneficial when applying these methods to complex control tasks which often require iterative optimization in a non-convex setting. In contrast, previous approaches are limited to fixed priors and hyperparameters, estimating the posterior state distribution using iterative relinearization of the dynamics [15], [19].

A. Contribution

Prior work proposed input inference for optimal control using open-loop optimization with linearization [16] and closed-loop optimization with expert controllers and covariance control [17]. This work provides a comprehensive review of the approach, with a novel analysis of the Gaussian control-inference duality through the posterior covariances and state-action value functions. Moreover, we compare the performance of different approximate inference techniques, and outline applications of our approach for high-dimensional and partially-observed model predictive control. We also discuss connections to risk-sensitive, maximum entropy and dual control; as well as optimization and exploration perspectives.

B. Related Work

Control-as-inference has been considered since the conception of modern optimal control, due to the concurrent development of linear quadratic regulator (LQR), Kalman filtering and linear quadratic regulator (LQG) [5], [20]. The revival in control-as-inference stems from simultaneous works that tackle the setting from different perspectives. Path integral control [4], [21], [22] exploits the duality between integration over trajectories and Monte Carlo expectations to derive a sample-based optimal control scheme that performs

adaptive importance sampling via stochastic perturbations. Linearly-solvable Markov decision processes [23] present a closely related approach, but in a discrete state space, where the disturbance assumption allows the problem to be solved as a linear program. Trans-dimensional Markov chain Monte Carlo [24] provides a principled means of performing sample-based finite-horizon optimal control that can jointly optimize the task horizon. Message passing methods [2], [3], [15], [25] allow the direct duality to be established between inference and dynamic programming-based control in discrete and continuous state spaces. In the Gaussian setting, there is a strong correspondence to the LQG problem [3], [15], and so approximate Gaussian inference similarly derives approximate inference control (AICO), an open-loop regularized Riccati equations nonlinear solver that resembles differential dynamic programming [26], specifically the Gauss-Newton approximation, i.e. iterative LQR (iLQR) [27], [28]. For nonlinear smoothing, AICO uses iterated inference, relinearizing about the posterior state mode each iteration. Posterior policy iteration (PPI) [19] extends AICO for feedback control, framing a linear Gaussian stochastic controller as a conditional distribution such that the posterior controls can be computed using the same iterated inference.

The inference perspective for control is strongly motivated by the reinforcement learning setting, which uses both optimal control and statistical methods [1], [29]–[31]. Furthermore, trajectory optimization has been regularized using information-geometric constraints, such as the Kullback-Leibler (KL) divergence [32]–[34], which can be interpreted as variational inference [35]. Inference methods have also been adopted for motion planning [36], applying optimized factor graph solvers to planning tasks [37].

Conversely, many techniques popularized by probabilistic inference have been applied independently to enhance optimal control. Extended LQR incorporates a filtering-like forward optimization into iLQR, [38], [39]. Quadrature methods have been adopted for trajectory optimization for greater accuracy [40]–[43]. Sampled differential dynamic programming uses Monte Carlo rollouts to accurately estimate value functions of non-smooth dynamics, by using relating the sample covariance to the inverse Hessian of the log-likelihood objective [44], [45]. Inference-based methods have also been used for model predictive control. Sequential Monte Carlo was used a sample-based solver for non-convex, non-Gaussian MPC [46]. Stein variational gradient descent has also been used to combine sample- and gradient-based computation for MPC to plan over multi-modal trajectories [47].

C. Notation

The matrix \mathbf{X}_1^T denotes a sequence of vectors $\{\mathbf{x}_1, \dots, \mathbf{x}_T\}$. For vectors $\mathbf{x}_1, \mathbf{x}_2$ and pos. def. matrix $\mathbf{S} \succ 0$ we define $\|\mathbf{x}_1 - \mathbf{x}_2\|_{\mathbf{S}}^2 = \frac{1}{2}(\mathbf{x}_1 - \mathbf{x}_2)^\top \mathbf{S}(\mathbf{x}_1 - \mathbf{x}_2)$. The probability of an event X is denoted by $\Pr(X)$. The expression $\mathbf{x} \sim p(\mathbf{x})$ means that a random variable $\mathbf{x} \in \mathbb{R}^n$ is distributed according to the density $p(\mathbf{x})$. The log-likelihood under this distribution is expressed as $\mathcal{L}(\mathbf{x}) = \log p(\mathbf{x})$. A multivariate Normal distribution with mean $\boldsymbol{\mu} \in \mathbb{R}^n$ and covariance $\boldsymbol{\Sigma} \in S_+^n$ is $\mathcal{N}(\boldsymbol{\mu}, \boldsymbol{\Sigma})$, where $+$ denotes positive (semi-)

definiteness. Normal and Gaussian are used interchangeably to refer to this distribution, and it is also presented in its *canonical* form $\mathcal{N}[\boldsymbol{\nu}, \boldsymbol{\Lambda}]$, where $\boldsymbol{\Lambda} = \boldsymbol{\Sigma}^{-1}$ and $\boldsymbol{\nu} = \boldsymbol{\Lambda}\boldsymbol{\mu}$. $\mathbb{E}[\mathbf{x}]$ and $\mathbb{V}[\mathbf{x}]$ denote the mean and covariance of \mathbf{x} respectively.

II. STOCHASTIC OPTIMAL CONTROL

Since the offspring of control, optimally controlling systems subject to stochastic disturbances have been examined, see e.g. [48]–[52]. In this section, we review relevant topics of stochastic optimal control (SOC) [53]. These topics are outlined in order to identify how inference can be used to perform optimal control. Specifically, we connect risk-sensitive linear quadratic dynamic programming to linear Gaussian Bayesian smoothing.

A. Finite-Horizon, Discrete-Time Optimal Control

We consider control of a stochastic, discrete-time, fully-observed, nonlinear, time-varying dynamical system, \mathbf{f}_t , with state $\mathbf{x} \in \mathbb{R}^{d_x}$ and input $\mathbf{u} \in \mathbb{R}^{d_u}$. For such a system, we desire the optimal controls over a horizon of T time steps that minimizes the time-varying cost functions $C_t : \mathbb{R}^{d_x} \times \mathbb{R}^{d_u} \rightarrow \mathbb{R}$ in expectation over the dynamics from an initial state \mathbf{x}_0 ,

$$\begin{aligned} \min_{\mathbf{U}_1^{T-1}} \quad & \mathbb{E}[C_T(\mathbf{x}_T) + \sum_{t=1}^{T-1} C_t(\mathbf{x}_t, \mathbf{u}_t)] \\ \text{s.t.} \quad & \mathbf{x}_{t+1} = \mathbf{f}_t(\mathbf{x}_t, \mathbf{u}_t) + \boldsymbol{\eta}_t, \quad \boldsymbol{\eta}_t \sim \mathcal{N}(\mathbf{0}, \boldsymbol{\Sigma}_{\boldsymbol{\eta}_t}). \end{aligned} \quad (1)$$

Various approaches to exactly or approximately solve this problem exist [53], [54]. The dynamic programming solution [54] introduces the state and state-action value functions V and Q , where

$$V_t(\mathbf{x}) = \min_{\mathbf{u}_t} Q_t(\mathbf{x}_t, \mathbf{u}_t), \quad V_T(\mathbf{x}_T) = C_T(\mathbf{x}_T), \quad \text{and} \quad (2)$$

$$Q_t(\mathbf{x}_t, \mathbf{u}_t) = \mathbb{E}[C_t(\mathbf{x}_t, \mathbf{u}_t) + V_{t+1}(\mathbf{f}_t(\mathbf{x}_t, \mathbf{u}_t))]. \quad (3)$$

We briefly summarize the linear quadratic Gaussian (LQG [50]), which we will use to identify the inference relations in the linear Gaussian setting. For compactness, we introduce the extended state-action vector $\boldsymbol{\tau}$, where $\boldsymbol{\tau} = [\mathbf{x} \ \mathbf{u}]^\top \in \mathbb{R}^{d_\tau}$.

In the case of LQR, the cost function is quadratic,

$$\begin{aligned} C_t(\mathbf{x}, \mathbf{u}) &= c_t + \mathbf{c}_t^\top \begin{bmatrix} \mathbf{x} \\ \mathbf{u} \end{bmatrix} + \begin{bmatrix} \mathbf{x} \\ \mathbf{u} \end{bmatrix}^\top \begin{bmatrix} \mathbf{C}_{\mathbf{x}\mathbf{x}_t} & \mathbf{C}_{\mathbf{x}\mathbf{u}_t} \\ \mathbf{C}_{\mathbf{x}\mathbf{u}_t}^\top & \mathbf{C}_{\mathbf{u}\mathbf{u}_t} \end{bmatrix} \begin{bmatrix} \mathbf{x} \\ \mathbf{u} \end{bmatrix}, \\ &= \boldsymbol{\tau}^\top \mathbf{C}_t \boldsymbol{\tau} + \mathbf{c}_t^\top \boldsymbol{\tau} + c_t, \quad \text{where } \mathbf{C}_t \succ 0 \ \forall t. \end{aligned}$$

The state-action value function is also quadratic,

$$\begin{aligned} Q_t(\mathbf{x}_t, \mathbf{u}_t) &= q_t + \mathbf{q}_t^\top \begin{bmatrix} \mathbf{x}_t \\ \mathbf{u}_t \end{bmatrix} + \begin{bmatrix} \mathbf{x}_t \\ \mathbf{u}_t \end{bmatrix}^\top \begin{bmatrix} \mathbf{Q}_{\mathbf{x}\mathbf{x}_t} & \mathbf{Q}_{\mathbf{x}\mathbf{u}_t} \\ \mathbf{Q}_{\mathbf{u}\mathbf{x}_t} & \mathbf{Q}_{\mathbf{u}\mathbf{u}_t} \end{bmatrix} \begin{bmatrix} \mathbf{x}_t \\ \mathbf{u}_t \end{bmatrix} \\ &= q_t + \mathbf{q}_t^\top \boldsymbol{\tau}_t + \boldsymbol{\tau}_t^\top \mathbf{Q}_t \boldsymbol{\tau}_t, \end{aligned}$$

as is the value function, $V_t(\mathbf{x}_t) = v_t + \mathbf{v}_t^\top \mathbf{x}_t + \mathbf{x}_t^\top \mathbf{V}_t \mathbf{x}_t$. The dynamics are affine Gaussian in the state,

$$\mathbf{x}_{t+1} = \mathbf{F}_t \begin{bmatrix} \mathbf{x}_t \\ \mathbf{u}_t \end{bmatrix} + \bar{\mathbf{f}}_t + \boldsymbol{\eta}_t, \quad \text{where } \mathbf{F}_t = [\mathbf{F}_{\mathbf{x}_t} \ \mathbf{F}_{\mathbf{u}_t}]. \quad (4)$$

The Q function update, (3), becomes

$$\mathbf{q}_t = \mathbf{c}_t + \mathbf{v}_{t+1} \mathbf{F}_{t+1}, \quad \mathbf{Q}_t = \mathbf{C}_t + \mathbf{F}_{t+1}^\top \mathbf{V}_{t+1} \mathbf{F}_{t+1}. \quad (5)$$

Using Q , the optimal control input is $\mathbf{u}_t^* = \arg \min_{\mathbf{u}_t} Q_t(\mathbf{x}_t, \mathbf{u}_t)$,

$$\mathbf{u}_t^* = -\mathbf{Q}_{\mathbf{u}\mathbf{u}_t}^{-1}(\mathbf{q}_{\mathbf{u}_t} + \mathbf{Q}_{\mathbf{u}\mathbf{x}_t} \mathbf{x}_t) = \mathbf{K}_t \mathbf{x}_t + \mathbf{k}_t = \boldsymbol{\pi}_t(\mathbf{x}_t), \quad (6)$$

yielding a time-varying linear control law. Substituting equation (6) into (2), the value function updates are

$$\mathbf{v}_t = \mathbf{q}_{\mathbf{x}_t} - \mathbf{q}_{\mathbf{u}_t}^\top \mathbf{Q}_{\mathbf{u}\mathbf{u}_t}^{-1} \mathbf{Q}_{\mathbf{u}\mathbf{x}_t}, \quad \mathbf{V}_t = \mathbf{Q}_{\mathbf{x}\mathbf{x}_t} - \mathbf{Q}_{\mathbf{x}\mathbf{u}_t} \mathbf{Q}_{\mathbf{u}\mathbf{u}_t}^{-1} \mathbf{Q}_{\mathbf{u}\mathbf{x}_t}. \quad (7)$$

Similar holds for the so-called differential dynamic programming solution, where the cost and dynamics are updated with a second-order Taylor approximation each iteration. The assumption of time-varying affine dynamics correspond to the so-called Gauss-Newton approximation [27], [28].

B. Risk-Sensitive Control

Introduced by Jacobson, risk-sensitive linear exponential quadratic Gaussian control [55], [56] derives a policy that, unlike LQG, is dependent on the severity of resulting uncertainty in the system dynamics. This risk sensitivity is determined by a scaling parameter $\sigma \in \mathbb{R}$ in a transformed objective,

$$-\frac{1}{\sigma} \log \mathbb{E} \left[\exp \left(-\sigma \left[C_T(\mathbf{x}_T) + \sum_{t=0}^{T-1} C_t(\mathbf{x}_t, \mathbf{u}_t) \right] \right) \right], \quad (8)$$

which results in the adjusted Bellman equation,

$$Q_t^\sigma(\mathbf{x}_t, \mathbf{u}_t) = C_t(\mathbf{x}_t, \mathbf{u}_t) + \frac{1}{\sigma} \log \mathbb{E}[\exp(-\sigma V_{t+1}(\mathbf{x}_{t+1}))].$$

The expectation results in a transformed value function V^σ

$$\exp(-\sigma V^\sigma(\mathbf{x})) = \int \exp(-\sigma V(\mathbf{x})) \mathcal{N}(\mathbf{x}; \boldsymbol{\mu}_x, \boldsymbol{\Sigma}_\eta) d\mathbf{x}.$$

For a quadratic model of V , this expectation is equivalent to adding two Gaussian random variables $\mathbf{V}_t^\sigma = (\boldsymbol{\Sigma}_{\eta_t} + \frac{1}{\sigma} \mathbf{V}_t^{-1})^{-1}$. The Q -function naturally has a similar adjustment, $\mathbf{Q}_t^\sigma = \mathbf{C}_t + \mathbf{F}_{t+1}^\top \mathbf{V}_t^\sigma \mathbf{F}_{t+1}$. As a result, the risk-sensitive optimal policy depends on the disturbance covariance. For $\sigma > 0$, the behavior is ‘risk seeking’. For $\sigma < 0$, the behavior is ‘risk averse’. As $\sigma \rightarrow 0$, we recover the nominal behavior, referred to as risk neutral. For a nonlinear system, an approximate optimal solution is optimized through linearization [57].

C. Covariance Control

While stochastic optimal control is typically concerned with optimizing the expected cost, methods have also been devised for controlling the state *distribution*. Covariance control [58] specifically looks at constraining the mean and covariance of the terminal state distribution to a target $p(\mathbf{x}_T^*)$. The linear Gaussian setting has been extensively studied, for both discrete [59] and continuous time [60], where it can be shown that a solution exists should the system be controllable and $\boldsymbol{\Sigma}_{\mathbf{x}_T^*} - \boldsymbol{\Sigma}_{\eta_T} \succeq 0$, given process noise covariance $\boldsymbol{\Sigma}_{\eta_t}$. The hard constraint can be tackled by decomposing the problem into feedforward control for the mean, and linear feedback control for the covariance [59]. The discrete-time case has correspondences to relative entropy minimization and minimum-energy LQG [59], [61], where the terminal cost corresponds to the Lagrange multiplier of the constraint. The nonlinear Gaussian case has been tackled using stochastic differential dynamic programming [62] and through the combination of sequential convex programs and statistical linearization [63]. The problem can also be viewed as a form of optimal transport

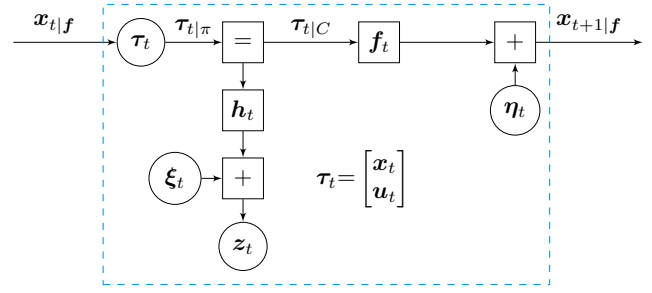


Fig. 1: Probabilistic graphical model of I2C for one timestep, following the notation of Loeliger *et al.* [65], illustrating how incorporating the quadratic cost structure yields a Gaussian state-space model for inference.

and the Schrödinger bridge, which seeks to find the mapping, i.e. dynamical system, that transforms one distribution into another [64].

III. INPUT INFERENCE FOR CONTROL

While progress has been made with respect to optimal control of systems subject to stochastic disturbances, progress is still hampered by the resulting required computations. Thus we now use the perspective of optimal control as input estimation to derive an inference procedure for optimal control which estimates the optimal state-action distribution.

A. Cost Functions and Constraints as Likelihoods

Control-as-inference techniques require a *belief in optimality* to perform optimal control [1], in order to construct a likelihood objective. Broadly, one can consider a binary random variable $\mathcal{O} \in \{0, 1\}$, for which 1 indicates optimality [30]. To ensure that a log-likelihood objective represents the cost, the exponential utility transform of the cost constructs a convenient likelihood [66]. The resulting density is a Boltzmann distribution and introduces an inverse ‘temperature’ α that scales the sharpness of this likelihood relative to the cost,

$$p(\mathcal{O}_t=1|\mathbf{x}_t, \mathbf{u}_t) \propto \exp(-\alpha C_t(\mathbf{x}_t, \mathbf{u}_t)). \quad (10)$$

As a result, the negative log-likelihood is an affine transform of the cost, which preserves convexity. In this work, we exploit the fact that a quadratic cost function¹ defined in a space $\mathbf{z} \in \mathbb{R}^{d_z}$ converts this distribution into a multivariate Normal, allowing approximate Gaussian inference methods to be used. We parameterize the quadratic cost as a distance from target state \mathbf{z}_t^* with weight $\boldsymbol{\Theta}_t$, where space \mathbf{z} is defined through a transform $\mathbf{h}_t(\mathbf{x}, \mathbf{u})$ of the state-action variables

$$C_t(\mathbf{x}_t, \mathbf{u}_t) = \|\mathbf{z}_t^* - \mathbf{h}_t(\mathbf{x}_t, \mathbf{u}_t)\|_{\boldsymbol{\Theta}_t}^2, \quad (11)$$

$$p(\mathcal{O}_t=1|\mathbf{x}_t, \mathbf{u}_t) = \mathcal{N}(\mathbf{z}_t = \mathbf{z}_t^* | \mathbf{x}_t, \mathbf{u}_t, \boldsymbol{\Theta}_t, \alpha). \quad (12)$$

When viewed as a state-space model, this is equivalent to a likelihood with a ‘measurement’ \mathbf{z}_t^* and ‘observation’ model

$$\mathbf{z}_t = \mathbf{h}_t(\mathbf{x}_t, \mathbf{u}_t) + \boldsymbol{\xi}_t, \quad \boldsymbol{\xi}_t \sim \mathcal{N}[\mathbf{0}, \alpha \boldsymbol{\Theta}_t]. \quad (13)$$

¹While we assume explicit quadratic structure here, a local quadratic approximation of an arbitrary cost function could also be used like in differential dynamic programming, i.e. the Laplace approximation of Equation 10 from the inference perspective [10].

Input: Probabilistic graphical model

$$p(\mathbf{Z}_1^T, \mathbf{X}_1^T, \mathbf{U}_1^{T-1}, \alpha_0), \text{ iterations } N$$

Output: Posterior controllers, $p(\mathbf{u}_t | \mathbf{x}_t, \mathbf{z}_{1:T})$

for $i \leftarrow 1$ **to** N **do**

 E-step: Bayesian smoothing to infer

$$p(\mathbf{X}_1^T, \mathbf{U}_1^{T-1} | \mathbf{Z}_1^T) \text{ given } \alpha_{i-1}, \text{ (Section III-B)}$$

 M-step: Update α_i and priors given

$$p(\mathbf{X}_1^T, \mathbf{U}_1^{T-1} | \mathbf{Z}_1^T)$$

end

Algorithm 1: Input inference for control

This motivates the use of Bayesian smoothing [67] to perform inference on this state-space model, despite considering a fully-observed problem, as the cost acts as an observation which guides the latent state-action trajectory towards optimality. This modeling assumption is motivated not only by the popularity of quadratic costs in optimal control; the resulting Gaussian cost likelihood yields a state-space model (Figure 1) that defines a finite-horizon inference problem (Equation 9) that can be tackled using approximate Gaussian inference, for which effective methods of analysis and computation are available [65], [67]. This inference problem evokes the use of the expectation maximization algorithm for dynamical system estimation [68], [69], but with the addition of input estimation [70]. In this case, the expectation maximization (EM) algorithm (Algorithm 1) consists of an E-step estimating the optimal state distribution given the cost and priors, and an M-step updating the priors and re-estimating the cost temperature α . This contrasts with prior work in which α is a constant hyperparameter, so only a single (but iterated) E-step is performed [19]. The perspective of input estimation, treating \mathbf{u} as a latent variable, provides a flexibility during inference that allows for both closed- and open-loop optimization and adaptive exploration. Therefore, we refer to this method as input inference for control (I2C).

The EM approach uses Bayes' rule to iteratively weigh the prior controller against the likelihood (i.e. control cost) to compute the posterior state-action distribution, which is the prior for the next iteration, as the dynamics and $p(\mathbf{x}_1)$ are fixed. This procedure is known as posterior policy iteration [19],

$$p_{i+1}(\mathbf{X}, \mathbf{U}) = p_i(\mathbf{X}, \mathbf{U} | \mathbf{Z}) \propto p_i(\mathbf{X}, \mathbf{U}) \exp(-\alpha \sum_t C_t(\mathbf{x}_t, \mathbf{u}_t)),$$

$$p_{i+1}(\mathbf{U} | \mathbf{X}) \propto p_i(\mathbf{U} | \mathbf{X}) \exp(-\alpha \sum_t C_t(\mathbf{x}_t, \mathbf{u}_t)).$$

The success of this procedure rests on three aspects: An initial prior $p_0(\mathbf{U} | \mathbf{X})$ that provides sufficient exploration, accurate inference to evaluate the controller, and an α that adequately calibrates the likelihood to effectively optimize under uncertainty by regularizing against greedy optimization.

B. Inference of Sequential Latent Variables

Factorizing the joint distribution into its Markovian structure (Equation 9) defines a graphical model that can be efficiently

solved using recursive Bayesian inference over time.

DEFINITION 1: GENERAL I2C INFERENCE

Control, where $p(\mathbf{u}_t | \mathbf{x}_t)$ is a stochastic control law $\pi_t(\mathbf{x})$

$$p(\mathbf{u}_t | \mathbf{x}_t, \mathbf{z}_{1:t-1}) \propto p(\mathbf{u}_t | \mathbf{x}_t) p(\mathbf{x}_t | \mathbf{z}_{1:t-1})$$

Forward optimization (innovation from the cost)

$$p(\mathbf{x}_t, \mathbf{u}_t | \mathbf{z}_{1:t}) \propto p(\mathbf{z}_t | \mathbf{x}_t, \mathbf{u}_t) p(\mathbf{x}_t, \mathbf{u}_t | \mathbf{z}_{1:t-1})$$

Dynamics prediction

$$p(\mathbf{x}_{t+1} | \mathbf{z}_{1:t}) = \int p(\mathbf{x}_{t+1} | \mathbf{x}_t, \mathbf{u}_t) p(\mathbf{x}_t, \mathbf{u}_t | \mathbf{z}_{1:t}) d\mathbf{x}_t d\mathbf{u}_t$$

Backward optimization (smoothing)

$$p(\mathbf{x}_t, \mathbf{u}_t | \mathbf{z}_{1:T}) = \int \left[\frac{p(\mathbf{x}_{t+1} | \mathbf{x}_t, \mathbf{u}_t) p(\mathbf{x}_{t+1} | \mathbf{z}_{1:T})}{p(\mathbf{x}_{t+1} | \mathbf{z}_{1:t})} \right] d\mathbf{x}_{t+1}$$

Note that I2C inference mirrors trajectory optimization, as both have a forward pass that simulates the current controller and a backward pass that acts to improve the trajectory. These steps are presented in Definition 1. While the equations are equivalent to Bayesian smoothing, the control step is unique to I2C, due to the latent variable being the joint state-action distribution.

C. The Gaussian Assumption

For tractability and convenience, we assume a Gaussian state-action distribution for the remainder of this article. As the central SOC problem (Equation 1) assumes a unique optimal trajectory, with approximate inference we use the Gaussian density to approximate the posterior about the maximum a posteriori solution. This assumption is supported by the Bernstein-von Mises theorem [71], which states a posterior will converge to a multivariate Normal about the maximum likelihood solution under certain regularity conditions. From the physical perspective, the Gaussian assumption of the dynamics disturbances and initial state distribution is supported by the central limit theorem [71]. The subsequent assumption of a Gaussian state-action trajectory is supported by adopting Gaussian controllers and the assumption that this dynamical system is adequately controlled, thus maintaining unimodality in the state distribution. Therefore, Gaussian I2C is limited to solving for the maximum a posteriori solution, and is unable to represent a more sophisticated controller than can reason over multimodal optimal trajectories. However, Gaussian filtering and smoothing has several attractive numerical qualities, namely exact inference in the linear setting, and well-developed approximate message passing techniques in the nonlinear setting [65], [67], [72]. Finally, Gaussians are convenient to marginalize and condition on, such that $p(\mathbf{u} | \mathbf{x})$ results

JOINT DISTRIBUTION OF THE PROBABILISTIC GRAPHICAL MODEL FOR OPTIMAL CONTROL

$$p(\mathbf{X}_1^T, \mathbf{U}_1^T, \mathbf{Z}_1^T, \alpha) = p(\mathbf{x}_1) \underbrace{p(\mathbf{z}_T | \mathbf{x}_T, \alpha)}_{\text{Terminal cost}} \prod_{t=1}^{T-1} \underbrace{p(\mathbf{x}_{t+1} | \mathbf{x}_t, \mathbf{u}_t)}_{\text{Dynamics}} \underbrace{p(\mathbf{z}_t | \mathbf{x}_t, \mathbf{u}_t, \alpha)}_{\text{Cost}} \underbrace{p(\mathbf{u}_t | \mathbf{x}_t)}_{\text{Controller}} \quad (9)$$

DEFINITION 2: GAUSSIAN I2C INFERENCE

Control, where $\pi_t(\mathbf{x}) = \mathcal{N}(\mathbf{K}_t^\pi \mathbf{x} + \mathbf{k}_t^\pi, \Sigma_t^\pi)$

$$\mathbf{K}_t^\pi := \Sigma_{\mathbf{u}_t} \Sigma_{\mathbf{x}_t}^{-1} \quad (14)$$

$$\mathbf{k}_t^\pi := \mu_{\mathbf{u}_t} - \mathbf{K}_t^\pi \mu_{\mathbf{x}_t}$$

$$\Sigma_t^\pi := \Sigma_{\mathbf{u}_t} - \Sigma_{\mathbf{u}_t} \Sigma_{\mathbf{x}_t}^{-1} \Sigma_{\mathbf{u}_t}^\top \quad (15)$$

$$\mu_{\mathbf{u}_t|\pi} = \mathbf{K}_t^\pi \mu_{\mathbf{x}_t|f} + \mathbf{k}_t^\pi$$

$$\Sigma_{\mathbf{u}_t|\pi} = \Sigma_t^\pi + \mathbf{K}_t^\pi \Sigma_{\mathbf{x}_t|f} \mathbf{K}_t^{\pi\top}$$

Forward optimization (innovation from the cost)

$$p(\tau_t|\pi) = p(\mathbf{x}_t, \mathbf{u}_t | \mathbf{z}_{1:t-1}) =$$

$$\mathcal{N}\left(\begin{bmatrix} \mu_{\mathbf{x}_t|f} \\ \mu_{\mathbf{u}_t|\pi} \end{bmatrix}, \begin{bmatrix} \Sigma_{\mathbf{x}_t|f} & \Sigma_{\mathbf{x}_t|f} \mathbf{K}_t^{\pi\top} \\ \mathbf{K}_t^\pi \Sigma_{\mathbf{x}_t|f} & \Sigma_{\mathbf{u}_t|\pi} \end{bmatrix}\right)$$

$$\mathbf{z}_t|\pi = \mathbf{h}_t(\tau_t|\pi) + \xi_t$$

$$p(\mathbf{z}_t|\pi, \tau_t|\pi) =$$

$$\mathcal{N}\left(\begin{bmatrix} \mu_{\mathbf{z}_t|\pi} \\ \mu_{\tau_t|\pi} \end{bmatrix}, \begin{bmatrix} \Sigma_{\mathbf{z}_t|\pi} & \Sigma_{\tau_t|\pi}^\top \\ \Sigma_{\tau_t|\pi} & \Sigma_{\tau_t|\pi} \end{bmatrix}\right) \quad (16)$$

$$\mathbf{K}_t^C := \Sigma_{\tau_t|\pi} \Sigma_{\mathbf{z}_t|\pi}^{-1} \quad (\text{Kalman gain}),$$

$$\mu_{\tau_t|C} = \mu_{\tau_t|\pi} + \mathbf{K}_t^C (\mathbf{z}_t - \mu_{\mathbf{z}_t|\pi})$$

$$\Sigma_{\tau_t|C} = \Sigma_{\tau_t|\pi} - \mathbf{K}_t^C \Sigma_{\mathbf{z}_t|\pi} \mathbf{K}_t^{C\top}$$

Dynamics prediction, where $\mathbf{x}_{t+1|f} = \mathbf{f}_t(\tau_t) + \eta_t$

$$p(\mathbf{x}_{t+1|f}, \tau_t) =$$

$$\mathcal{N}\left(\begin{bmatrix} \mu_{\mathbf{x}_{t+1|f}} \\ \mu_{\tau_t|C} \end{bmatrix}, \begin{bmatrix} \Sigma_{\mathbf{x}_{t+1|f}} & \Sigma_{\mathbf{x}_{t+1|f}\tau_t|C}^\top \\ \Sigma_{\mathbf{x}_{t+1|f}\tau_t|C} & \Sigma_{\tau_t|C} \end{bmatrix}\right) \quad (17)$$

Backward optimization (smoothing)

$$\mathbf{K}_t^s := \Sigma_{\mathbf{x}_{t+1|f}\tau_t|C}^\top \Sigma_{\mathbf{x}_{t+1|f}}^{-1}$$

$$\mu_{\tau_t|T} = \mu_{\tau_t|C} + \mathbf{K}_t^s (\mu_{\mathbf{x}_{t+1|f}} - \mu_{\mathbf{x}_{t+1|f}})$$

$$\Sigma_{\tau_t|T} = \Sigma_{\tau_t|C} + \mathbf{K}_t^s (\Sigma_{\mathbf{x}_{t+1|f}} - \Sigma_{\mathbf{x}_{t+1|f}}) \mathbf{K}_t^{s\top} \quad (18)$$

in time-varying linear (Gaussian) controllers. Therefore, while the Gaussian assumption is limiting, its locally linear quadratic approximations can be compared to linear quadratic optimal control approaches, which have been widely adopted.

Definition 2 describes the explicit message passing for Gaussian I2C from Definition 1. To compactly delineate each step, we use $t|\pi$, $t|C$ and $t|f$ to indicate a state after control, cost innovation and dynamics respectively. See Figure 1 for a factor graph visualization of the messages. As with standard Bayesian smoothing notation, t and $t|T$ describes the prior and posterior distribution. The initial state distribution is $\mathbf{x}_{1|f} \sim p(\mathbf{x}_1)$. Note, the computation of the joint distributions (Equations 16 and 17) depends on the chosen message passing method, which is approximate in the nonlinear setting (Section III-E). While Equations 14-18 are familiar to those experienced in Gaussian state estimation, it is not immediately clear from the expressions that this computation performs optimal control. To reveal this connection, we must consider the linear Gaussian setting and its duality to linear quadratic optimal control.

D. Linear Gaussian Inference & Linear Quadratic Control

In the case when the dynamics \mathbf{f} and the cost transform \mathbf{h} are affine transformations, the Gaussian message passing described in Section III-C can be performed exactly. Specifically, for notational simplicity we consider $C_t(\tau) = \|\tau_t^* - \tau\|_{C_t}^2$, and $\mathbf{x}_{t+1} = \mathbf{F}_t \tau_t + \bar{\mathbf{f}}_t + \eta_t$ as in Section II-A.

Exact message passing allows us to examine the inference computation in closer detail, and therefore concretely derive the correspondence to optimal control. However, in order to do this, we must first carefully distinguish the prior, likelihood and posterior, where the prior is the filtered distribution and the posterior is the smoothed distribution². Adopting notation from previous work [16], [65], we use \rightarrow for the prior and \leftarrow for the likelihood, so the posterior $p(\mathbf{x}) \propto p(\bar{\mathbf{x}})p(\check{\mathbf{x}})$, where

$$\Sigma = (\bar{\Lambda} + \check{\Lambda})^{-1} = \bar{\Sigma} - \bar{\Sigma}(\bar{\Sigma} + \check{\Sigma})^{-1}\check{\Sigma}. \quad (19)$$

Clearly recovering the optimal control expressions from the messages is challenging due to the nested regularization provided by the probabilistic computation. We use the relation between the Q -function and state-action log-likelihood as a compact alternative. To demonstrate this control equivalence, in the following passage we consider the limit where the prior becomes ‘uninformative’, that is $p(\mathbf{x}) \rightarrow p(\check{\mathbf{x}})$, and the dynamics deterministic ($\Sigma_{\eta_t} \rightarrow \mathbf{0}$). Numerically, uninformative priors occur when the relative uncertainty in the prior is significantly larger than the likelihood. We use \rightarrow in the following expressions to express this limiting case. Revisiting the smoothing step (18), using Woodbury’s inversion lemma [73], we can express the posterior using Equation 19 as

$$\Sigma_{\mathbf{x}_{t+1|T}} = \bar{\Sigma}_{\mathbf{x}_{t+1|f}} - \bar{\Sigma}_{\mathbf{x}_{t+1|f}} (\bar{\Sigma}_{\mathbf{x}_{t+1|f}} + \check{\Sigma}_{\mathbf{x}_{t+1}})^{-1} \check{\Sigma}_{\mathbf{x}_{t+1|f}}.$$

Substituting into the smoothing update (Equation 18),

$$\Sigma_{\tau_t|T} = \bar{\Sigma}_{\tau_t|C} - \bar{\Sigma}_{\tau_t|C} \mathbf{F}_t^\top (\bar{\Sigma}_{\mathbf{x}_{t+1|f}} + \check{\Sigma}_{\mathbf{x}_{t+1}})^{-1} \mathbf{F}_t \bar{\Sigma}_{\tau_t|C},$$

given $\mathbf{K}_t^s = \Sigma_{\tau_t|C} \mathbf{F}_t^\top \Sigma_{\mathbf{x}_{t+1|f}}^{-1}$ in the linear Gaussian setting. For affine dynamics, $\Sigma_{\mathbf{x}_{t+1|f}} = \mathbf{F}_t \Sigma_{\tau_t|C} \mathbf{F}_t^\top + \Sigma_{\eta_t}$, so we can use a matrix inversion identity³ [73] for $\Lambda_{\tau_t|T}$, where

$$\Lambda_{\tau_t|T} = \bar{\Lambda}_{\tau_t|C} + \mathbf{F}_t^\top (\Sigma_{\eta_t} + \check{\Sigma}_{\mathbf{x}_{t+1}})^{-1} \mathbf{F}_t. \quad (20)$$

The future state posterior can also be expressed as $\Sigma_{\mathbf{x}_{t+1|T}} = (\bar{\Sigma}_{\mathbf{x}_{t+1|f}}^{-1} + \check{\Sigma}_{\mathbf{x}_{t+1}}^{-1})^{-1}$, and given the uninformative prior $\Lambda_{\mathbf{x}_{t+1|T}} \rightarrow \Lambda_{\mathbf{x}_{t+1}}$. Moreover, from the innovation step during filtering $\Lambda_{\tau_t|C} = \Lambda_{\tau_t|\pi} + \alpha C_t$, and Σ_{η_t} is negligible for deterministic dynamics, Equation 20 reduces to

$$\Lambda_{\tau_t|T} \rightarrow \alpha C_t + \mathbf{F}_t^\top \Lambda_{\mathbf{x}_{t+1|T}} \mathbf{F}_t, \quad (21)$$

since $\bar{\Lambda}_{\tau_t|\pi}$ is uninformative. We can now identify Equation 21 as the Q update from Equation 5, with $\Lambda_{\tau_t|T} \equiv Q_t$ and $\Lambda_{\mathbf{x}_{t+1|T}} \equiv V_t$. Reflecting on the deterministic dynamics assumption where Σ_{η_t} is negligible, the reader may recognize that the $(\Sigma_{\eta_t} + \check{\Sigma}_{\mathbf{x}_{t+1}})^{-1} \rightarrow \Lambda_{\mathbf{x}_{t+1|T}}$ step is the same regularization introduced to the value function in the risk-sensitive

²Here, the prior at timestep t refers to the belief after inference forward in time for $1:t$ (i.e. filtering), while the posterior refers to the belief after inference over the whole trajectory $1:T$, which incorporates smoothing.

³ $A^{-1} - A^{-1}U(VA^{-1}U + B^{-1})^{-1}VA^{-1} = (A + UB^{-1}U)^{-1}$

formulation in Section II-B, $V_t^\sigma = (\Sigma_{\eta_t} + \frac{1}{\sigma} V_t^{-1})^{-1}$. We discuss this correspondence in more detail in Section V-2.

Having shown that the Gaussian posteriors relate to Q and V , we now illustrate the maximization step of dynamic programming through marginalization. For brevity, we drop the time index and conditioning indicator. To relate the conditional of the τ precision to the optimal linear feedback law, consider the block-wise inversion of the joint covariance

$$\begin{aligned} \Lambda_\tau &= \begin{bmatrix} \Sigma_x & \Sigma_{ux}^\top \\ \Sigma_{ux} & \Sigma_u \end{bmatrix}^{-1} = \begin{bmatrix} \Lambda_{xx} & \Lambda_{ux}^\top \\ \Lambda_{ux} & \Lambda_{uu} \end{bmatrix} \\ &= \begin{bmatrix} \Sigma_x^{-1} + \Sigma_x^{-1} \Sigma_{ux} \Sigma_*^{-1} \Sigma_{ux} \Sigma_x^{-1} & -\Sigma_x^{-1} \Sigma_{ux}^\top \Sigma_*^{-1} \\ -\Sigma_*^{-1} \Sigma_{ux} \Sigma_x^{-1} & \Sigma_*^{-1} \end{bmatrix} \end{aligned} \quad (22)$$

where $\Sigma_* = \Sigma_u - \Sigma_{ux} \Sigma_x^{-1} \Sigma_{ux}^\top$ (Schur complement), so

$$\begin{aligned} -\Lambda_{uu}^{-1} \Lambda_{ux} &\equiv -Q_{uu}^{-1} Q_{ux}, \\ &= \Sigma_* \Sigma_*^{-1} \Sigma_{ux} \Sigma_x^{-1} = \Sigma_{ux} \Sigma_x^{-1}. \end{aligned} \quad (23)$$

Therefore, Equation 23 relates the Q function-derived controller from Equation 6 to the i2C controller in Equation 14.

Finally, we use the joint precision in Equation 22 again to derive the value function update from Equation 7. The value function corresponds to the marginal of x from the joint. To understand its connection to the Q function, we consider the how the joint precision term Λ_{xx} in Equation 22 relates to the *marginal* state precision $\Sigma_x^{-1} = \Lambda_x$,

$$\Lambda_{xx} = \Sigma_x^{-1} + \Sigma_x^{-1} \Sigma_{ux} \Sigma_*^{-1} \Sigma_{ux} \Sigma_x^{-1} \quad (24)$$

$$\begin{aligned} &= \Lambda_x + \Lambda_{xu} \Lambda_{uu}^{-1} \Lambda_{ux}, \\ \therefore \Lambda_x &= \Lambda_{xx} - \Lambda_{xu} \Lambda_{uu}^{-1} \Lambda_{ux}, \end{aligned} \quad (25)$$

which corresponds to the V function update in Equation 7. As the dynamic programming method maintains a separate value and Q function, the value function is updated according to the equations in Equation 7. However, through manipulating the Gaussian distributions we can simply marginalize x from τ and compute Λ_x directly, and by working with the joint distribution throughout we avoid computing Q and V separately.

This analysis is closely related to the ‘soft’ Bellman backup from reinforcement learning [30], and the insight that a sample covariance approximates the inverse Hessian of its log-likelihood under the Gaussian assumption used in sampled differential dynamic programming [44].

E. Approximate Nonlinear Gaussian Inference

We now review methods for Gaussian message passing when the exact linear rules are not possible, as this is important for many interesting problems. To do so, we revisit the limiting assumption in Equation 21, and replace $h_t(\tau_t)$ with a locally linear approximation $H_t \tau_t + \bar{h}_t$, which may be obtained via function linearization or ‘statistical linearization’ using the quadrature or sample estimates. Using this linearized model, our equivalent cost coefficients should be transformed for optimizing τ , i.e. $C_t^\tau = H^\top C_t H$. Starting from the simplified Kalman update of $\Sigma_{\tau_t|C}$, using the matrix inverse identity³, we derive

$$\begin{aligned} \Sigma_{\tau_t|C} &= \Sigma_{\tau_t|\pi} - \Sigma_{\tau_t|\pi} H_t^\top (H \Sigma_{\tau_t|\pi} H_t^\top + \frac{1}{\alpha} C_\tau^{-1})^{-1} H_t \Sigma_{\tau_t|\pi} \\ \Lambda_{\tau_t|C} &= \Lambda_{\tau_t|\pi} + \alpha H_t^\top C_\tau H_t, \text{ as required.} \end{aligned}$$

Various approximation techniques for nonlinear Gaussian inference are available, compare Figure 2:

1) *Linearization*: Approximating the dynamics with a local linearization is attractive as it allows the linear Gaussian message passing rules to be adopted. Methods that adopt this approximation, such as the extended Kalman filter, are popular due to this convenience [74]. Like with differential dynamic programming, a second-order approximation can also be used, though this is costly. Local linearization approximations are limited in their accuracy, not only for highly nonlinear systems, but also for large state uncertainties. They typically require greater regularization or iterative computation to refine the linearization point. Moreover, while Jacobians can be straightforward to calculate, due to advancements in automatic differentiation, they are still $F_t \in \mathbb{R}^{d_x \times d_\tau}$ objects and therefore expensive to evaluate without optimized implementations. Linearization is also brittle numerically when applied to discontinuities such as constraints. Also, as with iLQR, EM with the linearization-based inference corresponds to Gauss-Newton optimization [75].

2) *Spherical Cubature Quadrature*: Quadrature rules construct evaluation points and weights in order to evaluate integrals for specific functions. For Gaussian densities, the 3rd order spherical cubature rule is popular [76], as it requires $2d$ points, scaling linearly with dimensionality d . This rule is also a special case of the unscented transform, popularized by the unscented Kalman filter [77]. The cubature quadrature rules are derived by computing ‘sigma’ points about the mean in each axis via the Cholesky decomposition of the covariance. The unscented transform includes the mean, and therefore requires $2d+1$ points, as well as two additional hyperparameters. While the unscented transform may provide an additional performance boost with hyperparameter tuning, we omit evaluation here and focus on the spherical cubature rules. Moreover, this rule relates to linearization through implicitly approximating the Jacobian via finite difference using the sigma points [78].

3) *Gauss-Hermite Quadrature*: While state estimation requires computationally efficient inference methods for real-time use, for ‘offline’ trajectory optimization we are able to invest computational cost for greater inference accuracy. There are many approaches for achieving this for Gaussian distributions. For example, Monte Carlo sampling will converge, regardless of state dimension, due to the central limit theorem. However, for time-series inference sequential Monte Carlo methods are preferred, and in practice we did not find the Monte Carlo inference to be numerically stable for the desired planning horizons. Continuing with the use of quadrature rules, Gauss-Hermite (G-H) rules [79] are designed integrals of the form $\int \exp(x^2) f(x) dx$, therefore appropriate for computing Gaussian moments. These rules are practically limited in the multivariate setting, as extending the quadrature points to a mesh results in exponential increase in points, d^p for state dimension d and degree p . We use it here as a baseline for accurate inference with i2C. The Gauss-Hermite message passing is the same as cubature quadrature, however the points and weights for a given degree must be obtained. Moreover, in the multivariate settings, the (1D) points and weights must

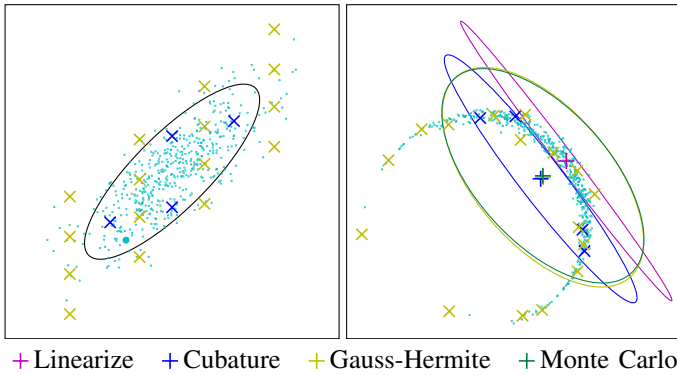


Fig. 2: An illustration of different approximate inference methods when propagating a bivariate Gaussian through a nonlinear function. The Monte Carlo samples (•) indicate the distribution becomes highly non-Gaussian, but evaluating these samples is computationally intensive. Linearizing the function returns an approximation that is highly localized around its (inaccurate) mean prediction. Cubature quadrature (+) uses $2d$ points, but improves the estimate, particularly in the mean. 4th-degree Gauss-Hermite (+) uses d^4 points, but almost directly matches the Monte Carlo estimate in mean and covariance.

be transformed to the appropriate mesh structure [67].

F. Expectation Maximization for Control

While the E-step returns an estimate of the optimal latent state-action distribution using Bayesian smoothing, the inverse temperature of the cost likelihood remains unknown. Prior approaches treat this term as a fixed constant [15], [25], many adopt an adaptive approach, such as by satisfying an explicit KL constraint [35]. We propose an alternative strategy where α is treated as an unknown model parameter, which we can optimize in the M-step of EM. This natural adaptivity removes the need to tune both α and the control prior as hyperparameters, as they jointly influence the E-step, and provides a means of automatically scaling this term for an arbitrary cost function. The question of which strategy is best ultimately rests on the underlying optimization problem. If the problem is convex (e.g. LQG), α can be fixed to a large value to avoid unnecessary regularization. For highly non-convex problems, this regularization is beneficial, but for weakly non-convex problems, tuning a constant α could outperform an adaptive strategy. There are also numerous alternative adaptive strategies, such as a linear schedule. In Section IV, this adaptive strategy is motivated in the context of Gauss-Newton optimization heuristics.

For Gaussian I2C, this expected log-likelihood is convex in α , which affords the closed-form update [16],

$$\alpha = \frac{(T-1)d_z + d_{z_T}}{\sum_t \text{tr}\{\Theta_t \mathbb{E}[\delta z_t \delta z_t^\top]\}}, \text{ where } \delta z_t = z_t^* - z_t. \quad (26)$$

As $\text{tr}\{\Theta_t \mathbb{E}[\delta z_t \delta z_t^\top]\} = \mathbb{E}[\delta z_t^\top \Theta_t \delta z_t]$, the expected cost, α is calibrated using the total trajectory cost averaged over the belief, time horizon and state dimensionality. During the M-step, we also update the control priors with the posterior $p(\mathbf{X}, \mathbf{U} | \mathbf{Z})$ for the next iteration.

In the nonlinear setting, this M-step is approximate as $\mathbb{E}[\delta z_t \delta z_t^\top]$ can not be computed exactly. Motivated by the idea of a regularized M-step, we restrict the update of α by applying a KL constraint to ξ , which can be shown to be equivalent to a ratio constraint on the α update [16]. As α is an inverse temperature, it controls the sharpness of the likelihood. For sufficiently stochastic problems, a sharp likelihood can lead to exploitation of the random dynamics disturbance, as the ‘signal-to-noise ratio’ of the simulated control belief against the dynamics noise makes it difficult to optimize the controls under the stochastic dynamics. This tendency to exploit uncertainty during optimization is coined ‘optimism’ [30]. Failing to regularize α can result in overly optimistic optimization, which can exploit state uncertainty arising from both the dynamics or approximate inference.

The complete I2C algorithm is summarized in Algorithm 1. The remaining hyperparameters to discuss are the control priors, specified for \mathbf{u} . These priors play a range of roles in the trajectory optimization and should be designed appropriately. Firstly they act as a learning rate, so lower variance priors will result in slower optimization. Secondly, they represent a source of entropy, so the variance also dictates the amount of possible exploration during optimization. Another design consideration is the nonlinearity of the system and inference choice, as the prior should be chosen to maintain the validity of the Gaussian assumption.

Regarding convergence guarantees, EM achieves monotonic improvement when inference is exact, and will converge to a unique optimum when the likelihood is convex [80]. When the E-step is approximate, likelihood optimality guarantees are limited by the inference accuracy [81]. This limitation motivates the adoption of Monte Carlo methods, as accuracy can be improved through a greater number of particles [69].

A discussion on the computational complexity of Gaussian I2C depends on the choice of inference method, but generally it is dominated by the matrix inversions of the largest covariance matrix. As the covariance inversion can be framed as solving a linear system with a positive definite matrix, the complexity is less severe than explicit inversion. Table II provides an empirical study of computational complexity for a complex dynamical system. It is also worth highlighting that the Bayesian smoothing approach adopted by I2C requires fewer inversions than the belief propagation approach proposed for PPI [19]. For a single forward and backward pass on a linear system, I2C is $\mathcal{O}(3d_x^3 + d_u^3)$ while PPI is $\mathcal{O}(7d_x^3 + 3d_u^3)$ if $d_z = d_x + d_u$.

G. Posterior Policy Iteration

Input inference for control can be viewed as an instantiations of approximate inference control [15] and posterior policy iteration [19], [25], as it estimates the posterior controller introduced in Section III-A using approximate inference. I2C is motivated as a cogent realization of this approach compared to the algorithmic definition of PPI (Algorithm 1, [19]) It is motivated closer to approximate Bayesian smoothing, rather than a regularized Riccati solver, to aid algorithmic developments and insights. The algorithmic realization of PPI fixes the prior controller, so only the posterior state trajectory is optimized using local linearization. However, for many

complex tasks, the posterior controller must be iteratively evaluated, e.g. due to actuator constraints. Secondly, using posterior linearizations for the subsequent forward pass, rather than directly evaluating the dynamics, has severely limited accuracy in practice when performing nonlinear trajectory optimization. Conversely, i2C considers the joint state-action distribution, so the dynamics and posterior controller are iteratively evaluated at each E-step. This realization enjoys a simpler implementation, fewer hyperparameters and lower computational complexity. This perspective, more grounded in approximate inference, aids translation into alternative inference techniques such as sequential Monte Carlo, and motivates connections to stochastic control, such as covariance control.

IV. APPROXIMATE INFERENCE FOR OPTIMIZATION

To clarify the difference between the expectation maximization proposed in Section III and the prior work that used iterative inference, we focus on the optimization perspective. To do so, we examine the simpler, but closely related, setting of a nonlinear inverse problem, to find input \mathbf{x} that maps to target \mathbf{y}^* through $\mathbf{f} : \mathbb{R}^{d_x} \rightarrow \mathbb{R}^{d_y}$, which is assumed differentiable, $\min_{\mathbf{x}} |\mathbf{y}^* - \mathbf{f}(\mathbf{x})|^2$. As before, we can optimize this problem using Gaussian inference, by framing it as a latent variable model with an unknown α , where the belief in \mathbf{x} is inferred iteratively

$$\mathbf{y}_i = \mathbf{f}(\mathbf{x}_i) + \boldsymbol{\xi}_i, \quad \mathbf{x}_i \sim \mathcal{N}(\boldsymbol{\mu}_i, \boldsymbol{\Sigma}_i), \quad \boldsymbol{\xi}_i \sim \mathcal{N}[\mathbf{0}, \alpha_i \mathbf{I}], \quad \alpha_i > 0.$$

This is closely related to Kalman optimization [82], which instead considers the more general optimization problem of $\nabla \mathbf{f} = 0$, but uses Gaussian inference in the same fashion. The posterior update evokes the Levenberg-Marquadt algorithm [83], a damped version of Gauss-Newton optimization, due to the regularization $\frac{1}{\alpha} \boldsymbol{\Sigma}_i^{-1}$ from the prior

$$\begin{aligned} \boldsymbol{\mu}_{i+1} &= \boldsymbol{\mu}_{\mathbf{x}|\mathbf{y}} = \boldsymbol{\mu}_i + \boldsymbol{\Sigma}_{\mathbf{x}\mathbf{y}} \boldsymbol{\Sigma}_{\mathbf{y}\mathbf{y}}^{-1} (\mathbf{y}^* - \hat{\mathbf{f}}(\boldsymbol{\mu}_i)), \\ &\approx \boldsymbol{\mu}_i + \left(\frac{1}{\alpha} \boldsymbol{\Sigma}_i^{-1} + \mathbf{J}_i^\top \mathbf{J}_i \right)^{-1} \mathbf{J}_i^\top (\mathbf{y}^* - \hat{\mathbf{f}}(\boldsymbol{\mu}_i)). \end{aligned}$$

Here, the crucial differences between iterative inference and EM can be made apparent. EM estimates \mathbf{J}_i during the forward pass, while iterative inference linearizes about $p(\mathbf{x}|\mathbf{y})$, requiring the additional hyperparameter θ and constructing a locally linear model for the surrogate model $\hat{\mathbf{f}}$.

$$\begin{aligned} \text{(It.) } \hat{\mathbf{f}}(\mathbf{x}) &= \mathbf{f}(\hat{\mathbf{x}}_i) + \mathbf{J}_i(\mathbf{x} - \hat{\mathbf{x}}_{i-1}), \quad \hat{\mathbf{x}}_i = \theta \hat{\mathbf{x}}_i + (1-\theta) \boldsymbol{\mu}_{\mathbf{x}|\mathbf{y}} \\ \text{(EM) } \hat{\mathbf{f}}(\mathbf{x}) &= \mathbf{f}(\mathbf{x}), \quad \mathbf{x}_i \sim p(\mathbf{x}|\mathbf{y}). \end{aligned}$$

Moreover, the need to iteratively tune α matches the similar heuristics used in Levenberg-Marquadt, and the behavior of Equation 26 also acts to reduce regularization as the cost reduces. Using a fixed α likely results in sub-optimal optimization without tuning. Posterior linearization also poses a practical problem for trajectory optimization, as the subsequent solution is not guaranteed to be close to the previous candidate. Therefore, a posterior linearization approach may likely produce an inaccurate state-action trajectory estimate compared to using the true function during filtering. To illustrate the importance of these differences empirically, we show the performance on a nonlinear, non-convex inverse problem shown in Figure 3. Comparing the equivalent approaches used by i2C

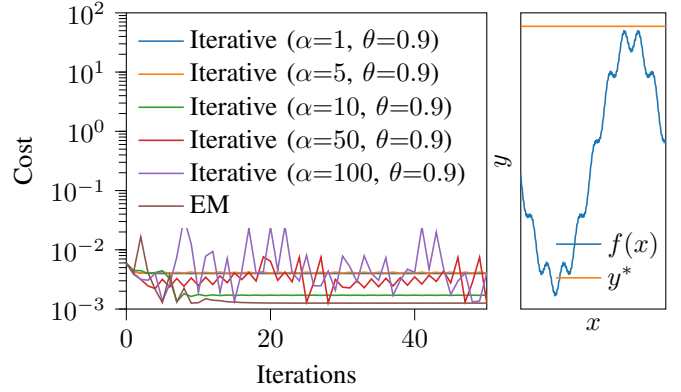


Fig. 3: For a 1D non-convex, nonlinear inverse problem, the adaptive regularization provided by the EM update rule can be shown to provide superior stability and convergence compared to fixed hyperparameters for iterative inference.

to AICO and PPI, we compare a fixed alpha with smoothing parameter θ to the EM approach (Equation 26). Sweeping through inverse temperatures, the solutions transition from sub-optimal to unstable. The EM approach automatically calculates adequate value for α to achieve superior convergence.

A. Note on Convergence

As a damped Gauss-Newton method, Gaussian i2C can be analyzed for local convergence under some conditions, but in general does not have guarantees for convergence [75]. A convergence analysis relates closely to that of Gauss-Newton methods [83], and more closely to the posterior linearization filter [84], which performs accurate Bayesian smoothing of Gaussian densities by iteratively re-linearizing about the posterior estimate. However, compared to state estimation, trajectory optimization is often initialized further from optimal trajectory, as the cost setpoints \mathbf{z}_i^* are often less informative of the optimal trajectory than sensor measurements, unless \mathbf{z}_i^* describes a tracking problem. Therefore, the convergence requirement that the initial solution is ‘sufficiently’ close to the fixed point is harder to guarantee in this setting, which reinforces the importance of the control priors and α to regularize against divergence. The posterior linearization filter analysis also highlights the importance of accurate inference for estimating the local likelihood curvature.

V. INTERPRETING INFERENCE-BASED CONTROL

Having demonstrated that Gaussian smoothing performs optimal control, we now discuss the additional benefits of inference-based control. This is illustrated by the likelihood objective (Equation 9), which contains additional regularization terms which can be connected to prior methods in control.

1) *Uncertainty-based Regularization*: An important aspect to i2C is how uncertainty influences the optimized control law. Most notable from Equation 14 is how the gain is attenuated by $\boldsymbol{\Sigma}_{\mathbf{x}_t}$, indicating that control action reduces with state uncertainty. This finding parallels the ‘turn-off phenomenon’ observed in dual control [85], [86] and Bayesian reinforcement learning [87], where actions are similarly attenuated under

model, and consequently state, uncertainty. For dual control, this regularization is detrimental due to the active learning component, however this behavior can be useful in settings such as model-based reinforcement learning [14], where regions of predictive uncertainty can indicate modeling error, and uncertainty-based regularization prevents these errors being exploited during optimization [88].

2) *Risk-Seeking Optimization*: Exponentiating the optimal control objective for risk sensitivity (Equation 8) has a clear connection to control-as-inference, due to the likelihood definition in Equation 10. As previous work has noted, this relates the risk coefficient σ to the inverse temperature α [19], [31], [35]. An immediate consequence of this is that $\sigma > 0$ for control-as-inference, so it is inherently ‘risk seeking’. Characterizing risk-seeking behavior as control attenuation, we can interpret this as a manifestation of the turn-off phenomena, as increasing σ acts to increase the state uncertainty. Interestingly, this presents risk-averse control as a counter to the turn-off phenomena, artificially reversing the regularization through the sign reversal of σ . The artificial nature of this mechanism is reflected in the numerical brittleness of risk-averse control, as it requires $\Sigma_{\eta_t} + \frac{1}{\sigma} \mathbf{V}_t^{-1}$ to be positive definite when $\sigma < 0$, which is difficult to ensure. Beyond attenuating feedback gains, I2C uses risk-seeking control in a secondary fashion due to the forward optimization during filtering. From the M-step update of I2C (Equation 26), we can see that as the average cost decreases, α increases and therefore the effective risk-seeking increases. To appreciate why it is beneficial for α to increase during optimization, and not simply remain fixed to a small, more risk neutral value, we must consider the expected log-likelihood objective. As α scales the control objective in the overall objective, a small α does not encourage optimization of the cost, while setting α high leads to overly aggressive forward optimization that neglects the dynamics likelihood, producing unfeasible trajectories. This ‘optimistic’ greediness, introduced in Section III-F, can prefer trajectories that violate the dynamics constraint, as $p(\mathbf{x}_{t+1}|\mathbf{x}_t, \mathbf{u}_t, \mathbf{z}_{1:t}) \neq p(\mathbf{x}_{t+1}|\mathbf{x}_t, \mathbf{u}_t)$ [30]. Conversely, the risk-neutral case turns off this forward optimization, removing the exploration mechanism. Therefore, I2C leverages risk-seeking optimization to accelerate convergence and the M-step can temper this exploration through adjusting α .

3) *Optimism as Exploration*: In this section, we briefly discuss the exploration benefits of inference-based control. The filtering operation during the forward pass has an exploratory effect, due to the interaction between the state uncertainty and the control cost when the state-action distribution is conditioned on the cost-as-likelihood. As a result, in the case of *epistemic* model uncertainty, this mechanism will prefer low-cost, uncertain regions of the state space. This strategy is reminiscent of the upper confidence bound (UCB) for ‘optimism under uncertainty’, an exploration strategy for bandit problems and Bayesian optimization (BO) [89]. When performing BO with a Gaussian process (GP), UCB optimizes for a confidence interval of the uncertain objective, defined through hyperparameter β . To compare the exploration strategies of UCB and filtering, we consider a simple bandit-like setting of optimizing a point estimate control u_0 for one timestep, given a GP

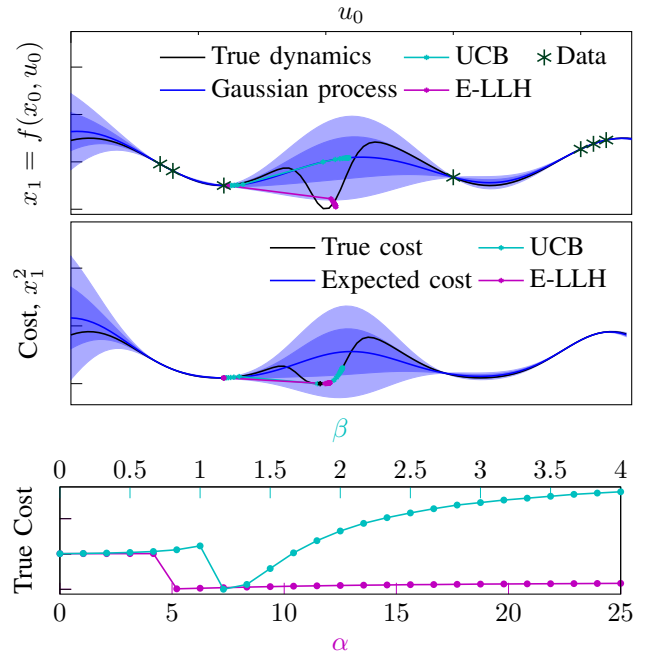


Fig. 4: A simple comparison between exploration using UCB and the expected log-likelihood (E-LLH) for a 1D Gaussian process dynamics model. UCB seeks the most uncertain region in the objective, while the inference-strategy seeks $x_1 = 0$ due to the cost-as-likelihood transformation and filtering step, such that the posterior x_1 drifts from the mean prediction. As a result, in this scenario, the inference approach selects an effective u_0 under uncertainty across a range of α values, while UCB tends to over-explore as β increases. Uncertainty intervals illustrate one and two standard deviations.

dynamics model $f(x, u) = \mathcal{N}(\mu(x, u), \sigma^2(x, u))$ and known starting state x_0 for a x_1^2 objective. The UCB objective is

$$\min_{u_0} \mathbb{E}[f(x_0, u_0)^2] - \beta \sqrt{\mathbb{V}[f(x_0, u_0)^2]}.$$

The inference approach involves filtering, computing the posterior $p(x_1)$, and optimizing the expected log-likelihood w.r.t. u_0 results in the following objective in u_0 ,

$$\min_{u_0} \alpha^2 (\mu_{x_1}^2 + \sigma_{x_1}^2) + \frac{1}{\sigma^2(x_0, u_0)} (\sigma_{x_1}^2 + (\mu_{x_1} - \mu(x_0, u_0))^2),$$

$$\mathcal{N}(\mu_{x_1}, \sigma_{x_1}^2) = \mathcal{N}\left(\frac{\mu(x_0, u_0)}{\alpha \sigma^2(x_0, u_0) + 1}, \frac{\sigma^2(x_0, u_0)}{\alpha \sigma^2(x_0, u_0) + 1}\right).$$

If $\alpha \sigma^2(x_0, u_0) \approx 0$, this objective minimizes the expected cost. As $\alpha \sigma^2(x_0, u_0)$ becomes large, optimizing for u_0 is no longer possible, as the state posterior will already be close to the optimal state by greedily exploiting uncertainty. Therefore, this objective considers the explorations-exploitation trade-off by balancing seeking sources of uncertainty to achieve greedy posterior updates against the resulting expected cost of the trajectory. Figure 4 shows how UCB and inference-based optimization differ in exploration strategy. While both methods optimize for the expected cost when exploration is not encouraged, UCB seeks high variance regions of the objective as β is increased. Conversely, in the inference setting u_0 is chosen so the state posterior achieves $x_1 = 0$ due to the informative structure of the cost likelihood.

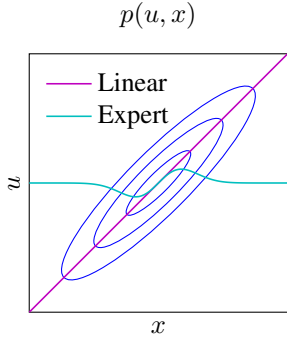


Fig. 5: The conditional Gaussian distribution as a linear control law. The standard linear control applies far outside the expected distribution, where it was not designed for. The ‘expert’ controller reverts to the prior when far from the mean, which prevents erroneous feedback control.

4) *Maximum Entropy Regularization:* The Gaussian assumption naturally incorporates its log-normalization terms into the log-likelihood, which for the Gaussian distribution is also its negative entropy. Augmenting the control objective with entropies evokes the maximum entropy (ME) principle, which has been applied to control for robustness, in particular for the controller in inverse optimal control [90]. The latent Gaussian prior on the controls adds ME regularization to i2C, which can be derived by examining the posterior policy. In explicit ME iLQG, the policy covariance takes the form $\Sigma_t = (C_{u_t} + F_{u_t}^\top V_{t+1} F_{u_t})^{-1}$ [91]. We can see from Q update in Equation 5 that this is the inverse of Q_{u_t} , and the expression for Σ_{u_t} in i2C (Equation 15) corresponds to the Schur complement form of Λ_{u_t} in Equation 22. As the stochastic aspect of the linear Gaussian controller is undesired in practice, the value of this ME regularization could be questioned. However, ME regularization was observed to influence desirable optimization behavior. For robust regions (e.g. where controls are clamped), the control variance was large, whereas at sensitive regimes (e.g. during energy injection in swing-up tasks) this variance was at a minimum. When updating u , a lower variance prior reduces the magnitude of the update, therefore for the robust and sensitive regions of the trajectory the control updates are regularized appropriately.

The α update in Equation 26 also has a ME interpretation. Following van Campenhout et al. [92], we can use the maximum entropy principle to motivate the cost likelihood.

Lemma 5.1: (Maximum entropy distributions, Section 12.1 [93]) Let function $\mathbf{h}(\mathbf{x}) : \mathbb{R}^{d_x} \rightarrow \mathbb{R}^h$ contain all ‘useful’ information about random variable \mathbf{x} . Given an observed empirical average $\hat{\mathbf{h}}$, and wish to find the density $q(\mathbf{x})$ such that $\int q(\mathbf{x})\mathbf{h}(\mathbf{x})d\mathbf{x} = \hat{\mathbf{h}}$. The maximum entropy distribution takes the form $q(\mathbf{x}) = Z^{-1} \exp(\lambda^\top \mathbf{h}(\mathbf{x}))$.

Proposition 5.1: Following Lemma 5.1, when the \mathbf{h} is a linear quadratic potential $h(\mathbf{x}) = \|\mathbf{z} - \mathbf{A}\mathbf{x}\|_Q^2$, where $\mathbf{z} \in \mathbb{R}^{d_z}$ and Q is symmetric positive definite, $q(\mathbf{x})$ is a multivariate Normal distribution. When \mathbf{A} is invertible, the expectation constraint can be satisfied when $\lambda = d_z/\hat{h}$.

This result matches Equation 26 for a single timestep with $\alpha = \lambda$, h as the control cost and \hat{h} obtained from the latent state-action trajectory. For the proof, refer to the Appendix. This perspective reflects how the cost is used to ‘summarize’ the state-action distribution. Moreover, α is introduced to satisfy a constraint, like in KL-regularized control [14], [32].

VI. EXTENSIONS & APPLICATIONS

This section presents several improvements and extensions to i2C for the stochastic control setting.

× \mathbf{x}_0 × \mathbf{x}_g —●— Closed-loop —○— Rollouts

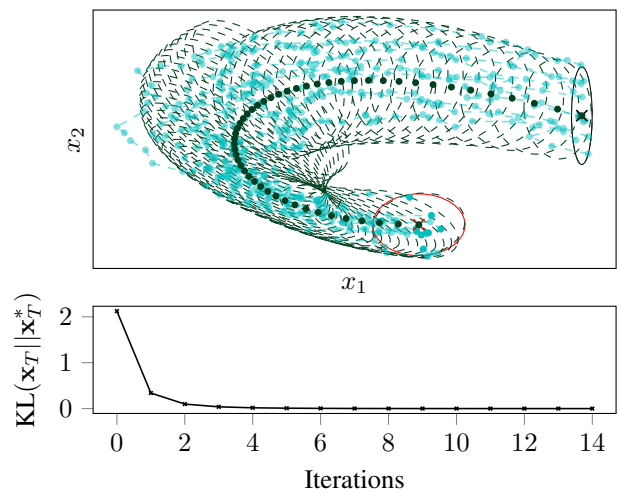


Fig. 6: i2C for exact minimum-energy linear Gaussian covariance control on an unstable system, with a fixed small α and $\Sigma_{\eta_t} = \text{diag}(0.1, 0.1)$. The KL divergence is between the terminal goal and closed-loop distributions.

A. Expert Linear Gaussian Controllers

A weakness of the Gaussian assumption made in Section III-C is the local nature of the estimate. Gaussian inference is equivalent to regularized local linearizations about the mean state-action trajectory. The local nature of this assumption introduces a brittleness to the control that limits its application in practical settings without additional modifications like re-planning, a limitation it shares with linearization-based control algorithms. Using inference, we can leverage the state belief to reduce this brittleness. In statistical machine learning, an *expert* is a model whose appropriateness applies to a specific portion of a state space [94]. We can incorporate this idea into the controller by switching between open- and closed-loop control using the predicted state distribution, (Figure 5),

$$\pi_t(\mathbf{u}|\mathbf{x}) = p_{\text{CL}} p(\mathbf{u}_t | \mathbf{x}_t) + (1-p_{\text{CL}})p(\mathbf{u}_t), \quad p_{\text{CL}} = \Pr(\mathbf{x}_t = \mathbf{x}).$$

For continuous random variables, $\Pr(\mathbf{x}_t = \mathbf{x})$ is an inconvenient quantity to compute. We take inspiration from outlier detection and define a suitable confidence interval. For a multivariate Normal distribution, our $\Pr(\mathbf{x}_t = \mathbf{x})$ can be computed using the Mahalanobis distance $d(\mathbf{x}) = \|\mathbf{x} - \boldsymbol{\mu}_{\mathbf{x}_t}\|_{\Sigma_{\mathbf{x}_t}^{-1}}^2$, which has a chi-square distribution. Using the cumulative density function $F_{\chi_k^2}$, $\Pr(\mathbf{x}_t = \mathbf{x}) = 1 - F_{\chi_k^2}(d(\mathbf{x}))$ [95]. For $k=2$, $\Pr(\mathbf{x}_t = \mathbf{x}) = \exp(-\frac{1}{2}d(\mathbf{x}))$, which works well and is convenient to compute as the unnormalized density of \mathbf{x}_t .

While this expert controller is valuable during optimization, it can also be used in execution, as it provides a degree of ‘safety’ by turning off feedback. However, there are also situations where this feedback relaxation impedes performance, such as unstable systems where high feedback is critical.

B. Covariance Control as Inference

In the standard i2C likelihood objective, the terminal cost is defined with a dedicated observation model $p(\mathbf{z}_T | \mathbf{x}_T)$. However, during inference we are also free to directly set the terminal latent state distribution before smoothing. In

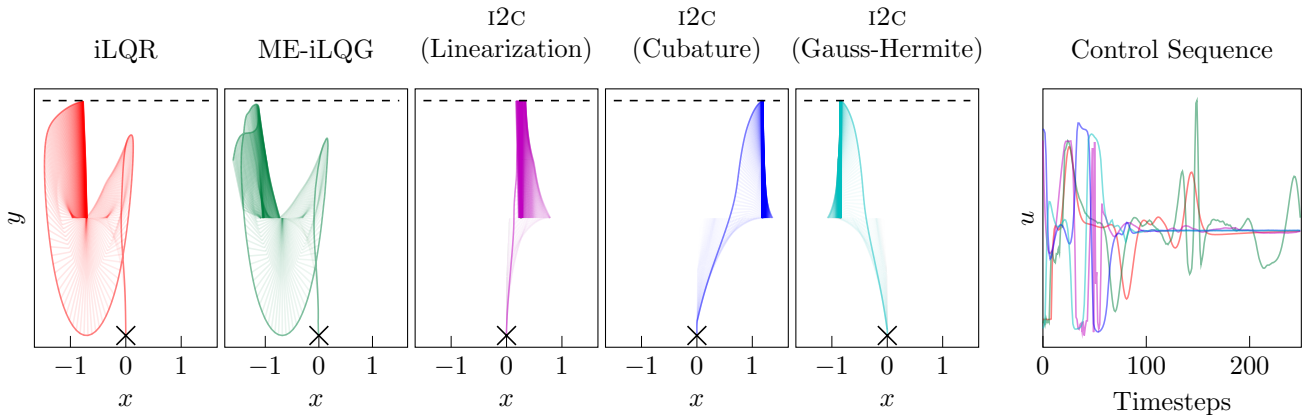


Fig. 7: Optimized trajectories of the double cartpole tip position, starting from \times . Note that the i2C variants return similar results due to shared hyperparameters. While the quadrature methods have cleaner trajectories due to the accuracy of their inference, that are remarkably similar given Gauss-Hermite requires much greater computation.

other timeseries inference settings such as state estimation, the terminal state posterior is set to the prior as there is no additional data to draw upon. However, for control we can avoid cost function design and the cost-to-likelihood translation by setting the terminal distribution directly. A downside of this approach is the requirement to stipulate the desired state directly rather than through a useful transformation that the cost usually provides. This approach is equivalent to covariance control (Section II-C) as iterations of forward and backward Riccati equations are performed until the boundary condition are satisfied. In this setting, Σ_{ξ_T} now acts as the Lagrange multiplier. Examining the expected log-likelihood term for the terminal state for the direct state optimization case $z_T = x_T + \xi_T$ [17], we see

$$\mathbb{E}[\log p(z_t | x_T) | x_T] \propto \|\mu_{z_T} - \mu_{x_T}\|_{\Sigma_{\xi}}^2 + \text{tr}\{\Sigma_{\xi_T}^{-1} \Sigma_{x_T}\} + \dots$$

which corresponds to the LQG correspondence proved in Equation 41 of Goldshtein et al. [59], where $\Sigma_{\xi_T}^{-1}$ is the terminal cost / Lagrange multiplier matrix. However, rather than compute this term, using our probabilistic framework we can set the terminal distribution directly via the posterior of x_T . In this case, the inference iteratively seeks to satisfy the boundary conditions on x_1 and x_T . Figure 6 demonstrates covariance control on a linear Gaussian system, where inference is exact. Note that i2C uses stochastic linear Gaussian controllers, whereas the previous literature solves the task using deterministic linear control. This variation of i2C naturally translates to nonlinear systems (Figure 8), avoiding the complexity of the additional forward sampling required for linearization-based covariance control [62]. However, the terminal boundary constraint still requires a means of being applied in an gradual manner, due to the iterative aspect of the nonlinear optimization. The terminal state distribution can be shifted from initially near the prior to the desired distribution by ‘annealing’ [96] the prior $p(\bar{x}_T)$ each iteration, i.e. $p(x_T) = p(x_T^*) p(\bar{x}_T)^\beta$ where $\beta \rightarrow 0$ following a linear schedule over iterations.

C. Integrating State Estimation and Control

As i2C uses recursive Bayesian estimation, it can be integrated seamlessly with state estimation algorithms, which correspond to the partially-observed optimal control problem. In the standard LQG problem, the separation principle applies

and the combination of a Kalman filter and LQR controller is optimal [53]. In the nonlinear setting, this convenient separation is no longer valid, however it is still applied in practice [28]. For i2C, the probabilistic graphical model is now extended to include a measurement model, i.e. $y_t = g_t(x) + \zeta_t$, $y \in \mathbb{R}^{d_y}$, $\zeta_t \sim \mathcal{N}(0, \Sigma_\zeta)$. Under this time-varying graphical model, the past and present state distribution is obtained using state estimation, so the planned controls must adapt to the updated state distribution at each timestep.

This replanning procedure naturally evokes model predictive control, which is also motivated by adapting optimal control to an evolving state distribution [97]. There is also a connection to dual control and the notion of closed-loop control vs. feedback control of Tse and Bar Shalom [98], as early work on replanning was motivated by reducing the adverse consequences of the turn-off phenomena (discussed in Section V.1) [98], [99].

VII. SIMULATED EXPERIMENTS

This section provides benchmarks of the i2C algorithm described in Section III as a trajectory optimization solver, as well as empirical investigations into the extensions discussed in Section VI: Expert-controllers and partially-observed MPC.

A. Approximate Inference for Control

In Section III-E, several approximate Gaussian message passing methods were discussed in order to apply Gaussian i2C to nonlinear systems. For this experiment, we evaluate each method on a deterministic double cartpole swing-up task. As a double cartpole is a chaotic nonlinear system where $\tau \in \mathbb{R}^7$, the degree of nonlinearity should challenge the accuracy of the approximate inference. As a baseline, we consider iLQR and maximum-entropy iLQG (denoted ME-iLQG) [32],

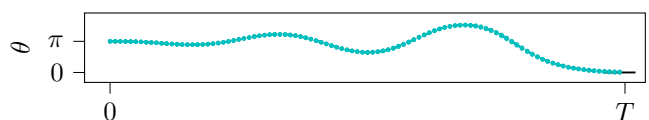


Fig. 8: Nonlinear minimum-energy covariance control on the pendulum swing-up task, using i2C with approximate inference. Plot depicts the inferred trajectory $---$ for target distribution $---$, with simulated rollouts $---$.

Environment	10th, 90th Cost Percentiles ($\times 10^3$)								
	i2c (S, E)	i2c (CE, E)	i2c (S, FF)	i2c (S, FB)	i2c (CE, FF)	i2c (CE, FB)	SQP (CE, FF)	iLQR (CE, FB)	ME-iLQG (S, FB)
Pendulum, $\tau \in \mathbb{R}^3$	13.46, 21.53	12.81, 17.11	17.72, 21.94	19.23, 21.43	13.97, 26.77	19.49, 22.31	18.10, 26.31	23.33, 26.46	19.45, 20.91
Cartpole, $\tau \in \mathbb{R}^5$	85.06, 87.43	81.83, 83.87	89.53, 94.67	93.53, 95.71	86.93, 89.75	121.89, 123.88	111.31, 118.57	142.23, 145.78	120.80, 122.45

TABLE I: The evaluation of SOC algorithms on finite-horizon, input-constrained control tasks. Variations are characterized by optimizing the stochastic (S) or certainty equivalent (CE) setting and using open-loop (FF), closed-loop (FB) or expert (E) controllers during optimization. These features identify similarities in performance. Percentiles were computed from 100 rollouts. SQP combines an open-loop trajectory optimized with sequential quadratic programming with local LQR feedback.

which use linearization-based approximations with line-search and relative entropy constrained updates respectively.

In order to demonstrate the consequences of approximate inference, we use the same priors and regularization across all i2C variants. In doing so, we show that i2C variations achieve similar high performance, but illustrate in Figure 9 how inference quality impacts optimization. Another important consideration is computation time. As discussed earlier, linearization-based approaches are unwieldy due to the Jacobian computation, especially for environments where Taylor approximations are not straightforward to compute. Moreover, iLQR requires line search for regularization which introduces additional computation. ME-iLQG uses cheaper, but usually conservative, KL regularization. The benefit of i2C is the adaptive regularization of the Bayes rule, which comes with the caveat of ‘optimistic exploration’. Moreover, the use of inference allows for greater flexibility in computation. Table II reports the average iteration time for double cartpole optimization. Note that the implementations of iLQR and ME-iLQG have optimized codebases, with pre-compiled Riccati equations and parallelized Jacobian computation. Despite this, iLQR is the most expensive, primarily due to the line search, as iterations were observed to be up to $\times 2$ faster than the average. ME-iLQG is faster than linearized i2C due to the ability to parallelize linearization, however cubature inference is the significantly faster method, as it balances computation and accuracy in a very attractive fashion in the nonlinear Gaussian setting. Moreover, while G-H is understandably the more expensive quadrature method, it was found to be faster than iLQR. Secondly, while G-H is clearly more accurate than cubature (e.g. Figure 2), the results in Figures 7 and 9 show that for double cartpole cubature gave sufficient accuracy.

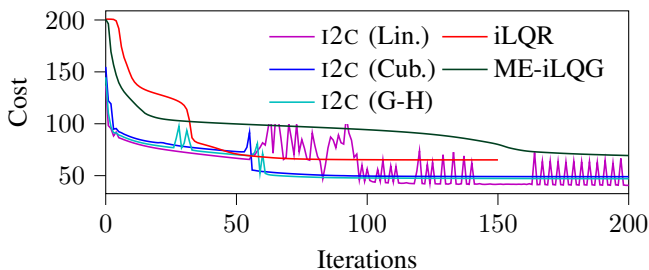


Fig. 9: Cost of the mean trajectory during trajectory optimization for double cartpole swing-up. While all i2C variants converge on similar solutions, the inaccuracy of linearization-based inference makes optimization more unstable. Figure 12 in the Appendix compared i2C performance over fixed values of α instead of the EM strategy.

B. Trajectory Optimization of Stochastic Systems

To evaluate the performance of the expert controller (Section VI-A), we consider two stochastic, nonlinear swing-up tasks against various open- and closed-loop baselines. The solvers also vary between considering the actual stochastic problem or a certainty equivalent approximation. In Table I we compare both i2C and baseline SOC solvers. For both tasks, open-loop methods resulted in better optima but were also high variance in the cost, while the closed-loop alternatives had much lower variance but sub-optimal performance on the simulated systems due to their over-actuation. Reassuringly, the results of the i2C variant and equivalent baseline solver were generally similar due to the comparable computation.

Incorporating the expert controller into the E-step softens the feedback control during exploration, effectively acting open-loop. This avoids highly-actuated trajectories forming, avoiding local optima. Table I demonstrates the effectiveness of this addition, where this expert controller matches the open-loop optima but with the closed-loop variance reduction.

C. High-Dimensional Model Predictive Control

For controlling complex, high-dimensional systems, local iterative solvers will struggle numerically when the task is highly non-convex and linearizations are not explicitly provided. We demonstrate the scalability of quadrature-based i2C on a challenging humanoid stand-up task, using MPC to amortize the difficult trajectory optimization. As a baseline, we consider sample-based MPC using the cross-entropy method (CEM) [100], an effective black-box optimization algorithm adopted for MPC [101]. CEM optimizes a factorized Gaussian distribution over action sequences, optimizing by moment matching the top performing Monte Carlo rollouts. The true cost is used, rather than the exponentiated form. As a result, CEM is free from the structure imposed by Gaussian message passing computation, but consequently suffers from high variance in the trajectories due to the Monte Carlo rollouts. Therefore, CEM provides an indication of the performance of the MAP solution using Monte Carlo computation, which in turn allows us to assess the effectiveness of the Gaussian approximate and quadrature inference of i2C.

The MPC algorithms are evaluated on a humanoid stand-up task using the MuJoCo simulator [102]. The humanoid has 17 actuators across 5 joints, and its state space (both intrinsic

	iLQR	ME-iLQG	i2C (Lin.)	i2C (Cub.)	i2C (G-H)
Time (s)	1.0	0.21	0.35	0.03	0.69

TABLE II: Relative computation time per iteration for double cartpole trajectory optimization, averaged over a maximum of 200 iterations and normalized about iLQR. G-H is degree 4.

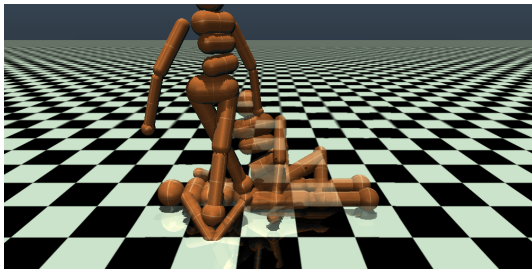


Fig. 10: Visualization of the humanoid standing trajectory with i2C MPC using cubature quadrature.

and extrinsic) is represented in \mathbb{R}^{27} . The task, depicted in Figure 10, requires control to stand to a height of 1.25m from rest in 1.8s, with a planning horizon of 0.72s represented as 30 control steps. Both methods share a control prior of $\Sigma_u = 0.1I$, as the actuators are limited to $[-1, 1]$, use 1 iteration per timestep and a warm-start of 50 iterations. For i2C, α is calibrated w.r.t. the prior and warm-start solution, but is kept fixed during execution as the optimization problem is non-stationary. Figure 10 demonstrates i2C MPC can successfully solve the task, and Table III shows that quadrature-based i2C inference is an effective use of particles, but superior performance can be obtained by CEM when significantly more samples are available. This suggests that a sequential Monte Carlo for i2C inference may be effective for such non-convex tasks.

D. Partially Observed Model Predictive Control

To investigate i2C MPC with state estimation, we compare cubature Gaussian i2C with iLQR for a 2D acrobatic quadcopter task ($x \in \mathbb{R}^6, u \in \mathbb{R}^2$), using a cubature Kalman filter for state estimation. Tracking a pre-specified trajectory, we evaluate the performance across increasing measurement uncertainty using the measurement model from Section VI-C. To simulate interesting state estimation dynamics, the positions and velocities of the left and right side of the copter in the world frame are measured. Therefore, during the somersault (Figure 11) the state uncertainty fluctuates, as the state is observed in a nonlinear manner.

We evaluate two measurement noise settings: low and high noise ($\Sigma_\zeta^{\text{low}}, \Sigma_\zeta^{\text{high}}$), where high noise masks out the velocities and right side position sensor. Low noise evaluates the methods for MPC, while the high noise case evaluates the effect of increased state uncertainty on i2C. iLQR is a deterministic, risk-neutral method, while i2C is probabilistic and risk-seeking, therefore we aim to understand how i2C uses of the state uncertainty from filtering and whether this aids control. Table IV discusses the results.

	i2C ($n=88$)	CEM ($n=50$)	CEM ($n=100$)	CEM ($n=500$)	CEM ($n=1000$)
Cost	47.78	105.28, 108.33	59.61, 62.82	42.55, 55.43	34.09, 51.72

TABLE III: Cost percentiles (10th, 90th) for the humanoid stand-up task over 25 seeds for MPC solvers with n particles. i2C is deterministic and requires $2d_{xu}$ points for inference. CEM demonstrates superior best-case performance, but only with significantly more rollouts.

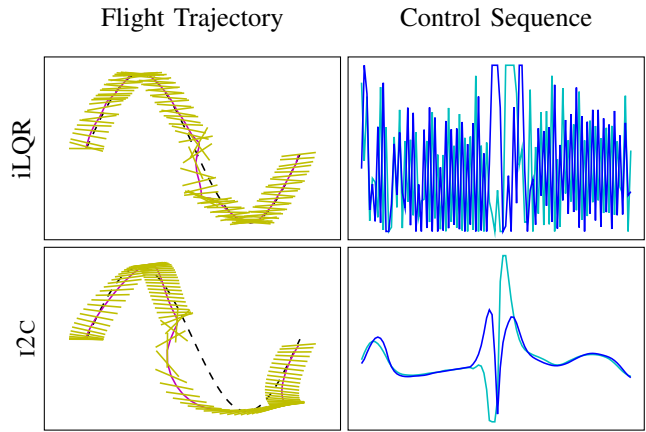


Fig. 11: Comparing the control of i2C and iLQR for an acrobatic quadcopter task, consisting of a smooth trajectory and 360° flip, under high measurement noise ($\Sigma_\zeta^{\text{high}}$). The trajectory is depicted by the desired and achieved trajectory, along with the measured pose. The controls consist of two thrusts applied to each end of the vehicle.

VIII. CONCLUSION

We have discussed how input estimation can be used to frame optimal control as an approximate inference problem. We have focused on the assumption of a Gaussian state-action distribution which, while having limited expressivity, provides the benefits of Gauss-Newton optimization and results in an uncertainty-regularized dynamic programming solver. While uncertainty-based regularization comes with (long-established) weaknesses, this approach has been demonstrated to be numerically competitive with popular solvers while also extending to alternative stochastic control methods like covariance control. Different approximation methods for Gaussian message passing were assessed and evaluated, comparing accuracy, computational cost and downstream control performance. Future work should consider relaxing the Gaussian assumption through methods such as sequential Monte Carlo [69], enabling multi-modal trajectory optimization.

Algorithm	10th, 90th Cost Percentiles	
	$\Sigma_\zeta^{\text{low}}$	$\Sigma_\zeta^{\text{high}}$
i2C (FF)	40.59, 41.52	113.35, 125.96
i2C (FB)	39.98, 41.03	113.41, 126.02
iLQR (FF)	111.73, 1968.39	107.02, 1809.36
iLQR (FB)	48.67, 68.35	53.85, 73.33

TABLE IV: Acrobatic quadcopter tracking performance under increasing state uncertainty over 50 random seeds. In the low noise setting, the i2C controller is superior and consistent across control modes. In the high noise setting, the increased states uncertainty induces i2C to regularize the control, leading to an increased cost that surpasses iLQR, but with reduced spread. This task setting illustrates when uncertainty-based regularization can be detrimental to performance.

REFERENCES

- [1] P. Dayan and G. E. Hinton, "Using expectation-maximization for reinforcement learning," *Neural Computation*, 1997.
- [2] H. Attias, "Planning by probabilistic inference," in *International Conference on Artificial Intelligence and Statistics*, 2003.
- [3] M. Toussaint and A. Storkey, "Probabilistic inference for solving discrete and continuous state Markov Decision Processes," in *International Conference of Machine Learning*, 2006.
- [4] H. J. Kappen, V. Gómez, and M. Opper, "Optimal control as a graphical model inference problem," in *International Conference on Automated Planning and Scheduling*, 2013.
- [5] R. E. Kalman, "A new approach to linear filtering and prediction problems," *Journal of basic Engineering*, 1960.
- [6] E. Todorov, "General duality between optimal control and estimation," in *IEEE Conference on Decision and Control*, 2008.
- [7] E. Theodorou and E. Todorov, "Relative entropy and free energy dualities: Connections to path integral and KL control," in *IEEE Conference on Decision and Control*, 2012.
- [8] P. Hennig, M. A. Osborne, and M. Girolami, "Probabilistic numerics and uncertainty in computations," *Proceedings of the Royal Society A: Mathematical, Physical and Engineering Sciences*, 2015.
- [9] A. Mesbah, "Stochastic model predictive control: An overview and perspectives for future research," *IEEE Control Systems Magazine*, 2016.
- [10] D. Barber, *Bayesian Reasoning and Machine Learning*. Cambridge University Press, 2011.
- [11] N. Matni, A. Proutiere, A. Rantzer, and S. Tu, "From self-tuning regulators to reinforcement learning and back again," in *IEEE Conference on Decision and Control*, 2019.
- [12] L. Hewing, K. P. Wabersich, M. Menner, and M. N. Zeilinger, "Learning-based model predictive control: Toward safe learning in control," *Annual Review of Control, Robotics, and Autonomous Systems*, 2020.
- [13] M. Maiworm, D. Limon, and R. Findeisen, "Online learning-based model predictive control with gaussian process models and stability guarantees," *International Journal of Robust and Nonlinear Control*, 2021.
- [14] M. P. Deisenroth, G. Neumann, J. Peters *et al.*, "A survey on policy search for robotics," *Foundations and Trends® in Robotics*, 2013.
- [15] M. Toussaint, "Robot trajectory optimization using approximate inference," in *International Conference on Machine Learning*, 2009.
- [16] J. Watson, H. Abdulsamad, and J. Peters, "Stochastic optimal control as approximate input inference," in *Conference on Robot Learning*, 2019.
- [17] J. Watson and J. Peters, "Advancing trajectory optimization with approximate inference: Exploration, covariance control and adaptive risk," in *American Control Conference*, 2021.
- [18] C. Hoffmann and P. Rostalski, "Linear optimal control on factor graphs - a message passing perspective -," *International Federation of Automatic Control*, 2017.
- [19] K. C. Rawlik, "On probabilistic inference approaches to stochastic optimal control," Ph.D. dissertation, The University of Edinburgh, 2013.
- [20] Y. Ho and R. Lee, "A Bayesian approach to problems in stochastic estimation and control," *IEEE Transactions on Automatic Control*, 1964.
- [21] H. J. Kappen and H. C. Ruiz, "Adaptive importance sampling for control and inference," *Journal of Statistical Physics*, 2016.
- [22] G. Williams, A. Aldrich, and E. A. Theodorou, "Model predictive path integral control: From theory to parallel computation," *Journal of Guidance, Control, and Dynamics*, 2017.
- [23] E. Todorov, "Linearly-solvable markov decision problems," in *Advances in Neural Information Processing Systems*, 2007.
- [24] M. Hoffman, A. Doucet, N. Freitas, and A. Jasra, "Bayesian policy learning with trans-dimensional MCMC," in *Advances in Neural Information Processing Systems*, 2008.
- [25] K. Rawlik, M. Toussaint, and S. Vijayakumar, "On stochastic optimal control and reinforcement learning by approximate inference," in *Robotics: Science and Systems*, 2012.
- [26] D. H. Jacobson and D. Q. Mayne, "Differential dynamic programming," 1970.
- [27] W. Li and E. Todorov, "Iterative linear quadratic regulator design for nonlinear biological movement systems," in *1st International Conference on Informatics in Control, Automation and Robotics*, 2004.
- [28] E. Todorov and W. Li, "A generalized iterative LQG method for locally-optimal feedback control of constrained nonlinear stochastic systems," in *American Control Conference*, 2005.
- [29] G. Neumann, "Variational inference for policy search in changing situations," in *International Conference on Machine Learning*, 2011.
- [30] S. Levine, "Reinforcement learning and control as probabilistic inference: Tutorial and review," *arXiv preprint arXiv:1805.00909*, 2018.
- [31] B. O'Donoghue, "Variational Bayesian reinforcement learning with regret bounds," *arXiv preprint arXiv:1807.09647*, 2018.
- [32] S. Levine and V. Koltun, "Guided policy search," in *International Conference on Machine Learning*, 2013.
- [33] R. Lioutikov, A. Paraschos, J. Peters, and G. Neumann, "Sample-based information-theoretic stochastic optimal control," in *IEEE International Conference on Robotics and Automation*, 2014.
- [34] H. Abdulsamad, O. Arenz, J. Peters, and G. Neumann, "State-regularized policy search for linearized dynamical systems," in *Proceedings of the International Conference on Automated Planning and Scheduling*, 2017.
- [35] S. Levine and V. Koltun, "Variational policy search via trajectory optimization," in *Advances in Neural Information Processing Systems*, 2013.
- [36] M. Mukadam, C.-A. Cheng, X. Yan, and B. Boots, "Approximately optimal continuous-time motion planning and control via probabilistic inference," in *IEEE International Conference on Robotics and Automation*, 2017.
- [37] M. Mukadam, J. Dong, X. Yan, F. Dellaert, and B. Boots, "Continuous-time Gaussian process motion planning via probabilistic inference," *The International Journal of Robotics Research*, 2018.
- [38] J. van den Berg, "Extended LQR: Locally-optimal feedback control for systems with non-linear dynamics and non-quadratic cost," in *Robotics Research*. Springer, 2016.
- [39] W. Sun, J. van den Berg, and R. Alterovitz, "Stochastic extended LQR for optimization-based motion planning under uncertainty," *IEEE Transactions on Automation Science and Engineering*, 2016.
- [40] E. Todorov and Y. Tassa, "Iterative local dynamic programming," in *Symposium on Adaptive Dynamic Programming and Reinforcement Learning*, 2009.
- [41] Y. Tassa, T. Erez, and W. Smart, "Receding horizon differential dynamic programming," in *Advances in Neural Information Processing Systems*, 2008.
- [42] Z. Manchester and S. Kuindersma, "Derivative-free trajectory optimization with unscented dynamic programming," in *IEEE Conference on Decision and Control*, 2016.
- [43] T. Howell, C. Fu, and Z. Manchester, "Direct policy optimization using deterministic sampling and collocation," *IEEE Robotics and Automation Letters*, 2021.
- [44] J. Rajamäki, K. Naderi, V. Kyrki, and P. Hämmäläinen, "Sampled differential dynamic programming," in *IEEE International Conference on Intelligent Robots and Systems*, 2016.
- [45] J. Rajamäki and P. Hämmäläinen, "Regularizing sampled differential dynamic programming," in *American Control Conference*, 2018.
- [46] N. Kantas, J. Maciejowski, and A. Lecchini-Visintini, "Sequential monte carlo for model predictive control," in *Nonlinear model predictive control*, 2009.
- [47] A. Lambert, A. Fishman, D. Fox, B. Boots, and F. Ramos, "Stein variational model predictive control," in *Conference on Robot Learning*, 2020.
- [48] A. Charnes and W. W. Cooper, "Deterministic equivalents for optimizing and satisficing under chance constraints," *Operations research*, 1963.
- [49] K. J. Åström, *Introduction to stochastic control theory*. Courier Corporation, 2012.
- [50] A. E. Bryson, *Applied optimal control: Optimization, estimation and control*. Routledge, 2018.
- [51] A. Mesbah, S. Streif, R. Findeisen, and R. D. Braatz, "Stochastic nonlinear model predictive control with probabilistic constraints," in *American control conference (ACC)*. IEEE, 2014.
- [52] J. A. Paulson, A. Mesbah, S. Streif, R. Findeisen, and R. D. Braatz, "Fast stochastic model predictive control of high-dimensional systems," in *53rd IEEE Conference on decision and Control*. IEEE, 2014, pp. 2802–2809.
- [53] R. F. Stengel, *Stochastic optimal control: Theory and application*. John Wiley & Sons, Inc., 1986.
- [54] D. P. Bertsekas and S. E. Shreve, *Stochastic optimal control: the discrete-time case*. Athena Scientific, 1996.
- [55] D. Jacobson, "Optimal stochastic linear systems with exponential performance criteria and their relation to deterministic differential games," *IEEE Transactions on Automatic Control*, 1973.
- [56] P. Whittle, "Risk-sensitive linear/quadratic/Gaussian control," *Advances in Applied Probability*, 1981.

- [57] F. Farshidian and J. Buchli, "Risk sensitive, nonlinear optimal control: Iterative linear exponential-quadratic optimal control with Gaussian noise," *arXiv preprint arXiv:1512.07173*, 2015.
- [58] A. F. Hotz and R. E. Skelton, "A covariance control theory," in *IEEE Conference on Decision and Control*, 1985.
- [59] M. Goldshtein and P. Tsiotras, "Finite-horizon covariance control of linear time-varying systems," in *IEEE Conference on Decision and Control*, 2017.
- [60] Y. Chen, T. T. Georgiou, and M. Pavon, "Optimal steering of a linear stochastic system to a final probability distribution, part i," *IEEE Transactions on Automatic Control*, 2016.
- [61] A. Beghi, "On the relative entropy of discrete-time markov processes with given end-point densities," *IEEE Transactions on Information Theory*, 1996.
- [62] Z. Yi, Z. Cao, E. Theodorou, and Y. Chen, "Nonlinear covariance control via differential dynamic programming," in *American Control Conference*, 2020.
- [63] E. Bakolas and A. Tsolovikos, "Greedy finite-horizon covariance steering for discrete-time stochastic nonlinear systems based on the unscented transform," in *American Control Conference*, 2020.
- [64] Y. Chen, "Modeling and control of collective dynamics: From schrödinger bridges to optimal mass transport," Ph.D. dissertation, University of Minnesota, 2016.
- [65] H.-A. Loeliger, J. Dauwels, J. Hu, S. Korl, L. Ping, and F. R. Kschischang, "The factor graph approach to model-based signal processing," *Proceedings of the IEEE*, 2007.
- [66] J. Peters and S. Schaal, "Reinforcement learning by reward-weighted regression for operational space control," in *International Conference on Machine Learning*, 2007.
- [67] S. Särkkä, *Bayesian Filtering and Smoothing*. Cambridge University Press, 2013.
- [68] R. H. Shumway and D. S. Stoffer, "An approach to time series smoothing and forecasting using the EM algorithm," *Journal of time series analysis*, 1982.
- [69] T. B. Schön, A. Wills, and B. Ninness, "System identification of nonlinear state-space models," *Automatica*, 2011.
- [70] L. Bruderer, "Input estimation and dynamical system identification: New algorithms and results," Ph.D. dissertation, ETH Zurich, 2015.
- [71] A. W. v. d. Vaart, *Asymptotic Statistics*. Cambridge University Press, 1998.
- [72] E. Petersen, C. Hoffmann, and P. Rostalski, "On approximate nonlinear Gaussian message passing on factor graphs," in *2018 IEEE Statistical Signal Processing Workshop*, 2018.
- [73] K. B. Petersen, M. S. Pedersen *et al.*, "The matrix cookbook," *Technical University of Denmark*, 2008.
- [74] B. D. Anderson and J. B. Moore, *Optimal filtering*, 2012.
- [75] B. M. Bell, "The iterated Kalman smoother as a Gauss-Newton method," *SIAM Journal on Optimization*, 1994.
- [76] I. Arasaratnam and S. Haykin, "Cubature Kalman filters," *IEEE Transactions on Automatic Control*, 2009.
- [77] S. J. Julier and J. K. Uhlmann, "New extension of the Kalman filter to nonlinear systems," in *Signal Processing, Sensor Fusion, and Target Recognition VI*. International Society for Optics and Photonics, 1997.
- [78] T. S. Schei, "A finite-difference method for linearization in nonlinear estimation algorithms," *Automatica*, 1997.
- [79] K. Ito and K. Xiong, "Gaussian filters for nonlinear filtering problems," *IEEE Transactions on Automatic Control*, 2000.
- [80] C. F. J. Wu, "On the Convergence Properties of the EM Algorithm," *The Annals of Statistics*, 1983.
- [81] A. Gunawardana and W. Byrne, "Convergence theorems for generalized alternating minimization procedures," *Journal of Machine Learning Research*, 2005.
- [82] A. F. García-Fernández and L. Svensson, "Gaussian map filtering using Kalman optimization," *IEEE Transactions on Automatic Control*, 2015.
- [83] R. Fletcher, *Practical Methods of Optimization*. John Wiley & Sons, 1987.
- [84] A. F. García-Fernández, L. Svensson, and S. Särkkä, "Iterated posterior linearization smoother," *IEEE Transactions on Automatic Control*, 2017.
- [85] M. Aoki, *Optimization of stochastic systems: topics in discrete-time systems*. Academic Press, 1967, vol. 32.
- [86] Y. Bar-Shalom, "Stochastic dynamic programming: Caution and probing," *IEEE Transactions on Automatic Control*, 1981.
- [87] E. D. Klenske and P. Hennig, "Dual control for approximate Bayesian reinforcement learning," *Journal of Machine Learning Research*, 2016.
- [88] J. G. Schneider, "Exploiting model uncertainty estimates for safe dynamic control learning," *Advances in Neural Information Processing Systems*, 1997.
- [89] N. Srinivas, A. Krause, S. Kakade, and M. Seeger, "Gaussian process optimization in the bandit setting: No regret and experimental design," in *International Conference on Machine Learning*, 2010.
- [90] B. D. Ziebart, "Modeling purposeful adaptive behavior with the principle of maximum causal entropy," Ph.D. dissertation, Carnegie Mellon University, 2010.
- [91] S. Levine, "Motor skill learning with local trajectory methods," Ph.D. dissertation, Stanford University, 2014.
- [92] J. van Campenhout and T. Cover, "Maximum entropy and conditional probability," *IEEE Transactions on Information Theory*, 1981.
- [93] T. M. Cover and J. A. Thomas, *Elements of Information Theory*. Wiley-Interscience, 2006.
- [94] I. C. Gormley and S. Frühwirth-Schnatter, "Mixture of experts models," in *Handbook of mixture analysis*. Chapman and Hall/CRC, 2019.
- [95] R. Johnson and D. Wichern, *Applied multivariate statistical analysis*, 2002.
- [96] N. Ueda and R. Nakano, "Deterministic annealing variant of the EM algorithm," in *Neural Information Processing Systems*, 1994.
- [97] "Model predictive control: past, present and future," *Computers & Chemical Engineering*, 1999.
- [98] Y. Bar-Shalom and E. Tse, "Dual effect, certainty equivalence, and separation in stochastic control," *IEEE Transactions on Automatic Control*, 1974.
- [99] R. Curry, "A new algorithm for suboptimal stochastic control," *IEEE Transactions on Automatic Control*, 1969.
- [100] R. Y. Rubinstein and D. P. Kroese, *The Cross Entropy Method: A Unified Approach To Combinatorial Optimization, Monte-Carlo Simulation (Information Science and Statistics)*, 2004.
- [101] N. Wagener, C. an Cheng, J. Sacks, and B. Boots, "An online learning approach to model predictive control," in *Robotics: Science and Systems*, 2019.
- [102] E. Todorov, T. Erez, and Y. Tassa, "Mujoco: A physics engine for model-based control," in *IEEE International Conference on Intelligent Robots and Systems*, 2012.
- [103] A. Mathai and S. Provost, *Quadratic Forms in Random Variables: Theory and Applications*, 1992.

APPENDIX

Experimental details can be found in the codebase

www.github.com/JoeMWatson/input-inference-for-control.

A. Proof for Proposition 5.1

Proof: When h is the linear quadratic potential $\|z - Ax\|_Q^2$, where A is invertible and Q is symmetric pd, $q(x)$ is Gaussian with the moments $q(x) = \mathcal{N}(\mu_q, \Sigma_q) = \mathcal{N}((\bar{A}^T \bar{A})^{-1} \bar{A}^T Pz, \frac{1}{\lambda} (\bar{A}^T \bar{A})^{-1})$, where $\bar{A} = PA$, using the Cholesky decomposition of $Q = P^T P$. Following the quadratic form for Gaussian variables, the expected cost under q can be expressed as [103] $\mathbb{E}_{x \sim q(\cdot)}[h(x)] = \text{tr}\{QA\Sigma_q A^T\} + (z - A\mu_q)^T Q(z - A\mu_q)$. The right term is zero as $A\mu_q = A(PA)^{-1}Pz = z$. The trace simplifies to $\text{tr}\{QA\Sigma_q A^T\} = \text{tr}\{\bar{A}^T \bar{A}\Sigma_q\} = d_z/\lambda$. Therefore, to satisfy the expectation constraint, $\lambda = d_z/\bar{h}$. ■

B. Additional Results

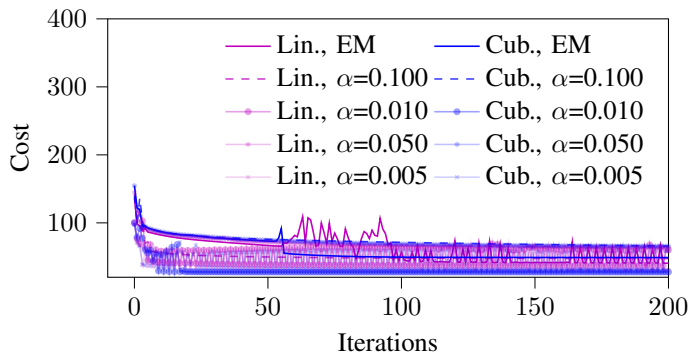


Fig. 12: Revisiting the experiment of Figure 9 to compare approximate inference against α strategy. As illustrated in Section IV, a fixed α can often lead to sub-optimal convergence or numerical stability. EM-based adaptive tuning automatically scales the hyperparameter to aid stability and performance. As illustrated in this task, careful optimization of a fixed α can result in superior performance when combining aggressive optimization with more accurate inference.



Joe Watson received a BA and MEng in Information and Computer Engineering from Peterhouse, University of Cambridge in 2016, where he was the Charles Babbage Senior Scholar. He is currently working towards a PhD degree with the Intelligent Autonomous Systems Group, Computer Science Department, Technical University of Darmstadt. He is broadly interested in the intersection of control and probabilistic inference for sample-efficient learning algorithms for robotics.



Hany Abdulsamad is a postdoctoral researcher at Aalto University and the Finnish Center for Artificial Intelligence. He completed his PhD degree with the Intelligent Autonomous Systems Group, Computer Science Department, Technical University of Darmstadt. Hany's research considers the intersection of statistical inference and control, focusing on switching linear dynamics and hybrid systems.



Rolf Findeisen is a full professor and heads the Control and CyberPhysical Systems Laboratory at the Technical University of Darmstadt. He received the M.S. degree from the University of Wisconsin, Madison, and the Ph.D. degree from the University of Stuttgart. Rolf was a research assistant in the Automatic Control Laboratory, ETH Zürich, and had several research stays and guest professorships, including Massachusetts Institute of Technology, Cambridge, USA, EPF Lausanne, Imperial College London.

Before moving the TU Darmstadt, he headed the Systems Theory and Control Laboratory at the Otto von Guericke University Magdeburg. His research interests focus on the model predictive control, the fusion of control and learning with guarantees, control of interconnected systems, and cyber-physical and network-controlled systems. The main fields of applications span mechatronics, robotics, autonomous driving to synthetic biology. Dr. Findeisen was the IPC Chair of the IFAC World Congress 2021. He has been an editor and associate editor for several journals, including the IEEE Transactions on Control of Network System and the IEEE Control Systems Magazine.



Jan Peters is a full professor (W3) for Intelligent Autonomous Systems at the Computer Science Department of the Technical University of Darmstadt. Jan Peters has received the Dick Volz Best 2007 US Ph.D. Thesis Runner-Up Award, the Robotics: Science & Systems - Early Career Spotlight, the INNS Young Investigator Award, and the IEEE Robotics & Automation Society's Early Career Award as well as numerous best paper awards. In 2015, he received an ERC Starting Grant and in 2019, he was appointed

as an IEEE Fellow.